CHALMERS
UNIVERSITY OF TECHNOLOGY

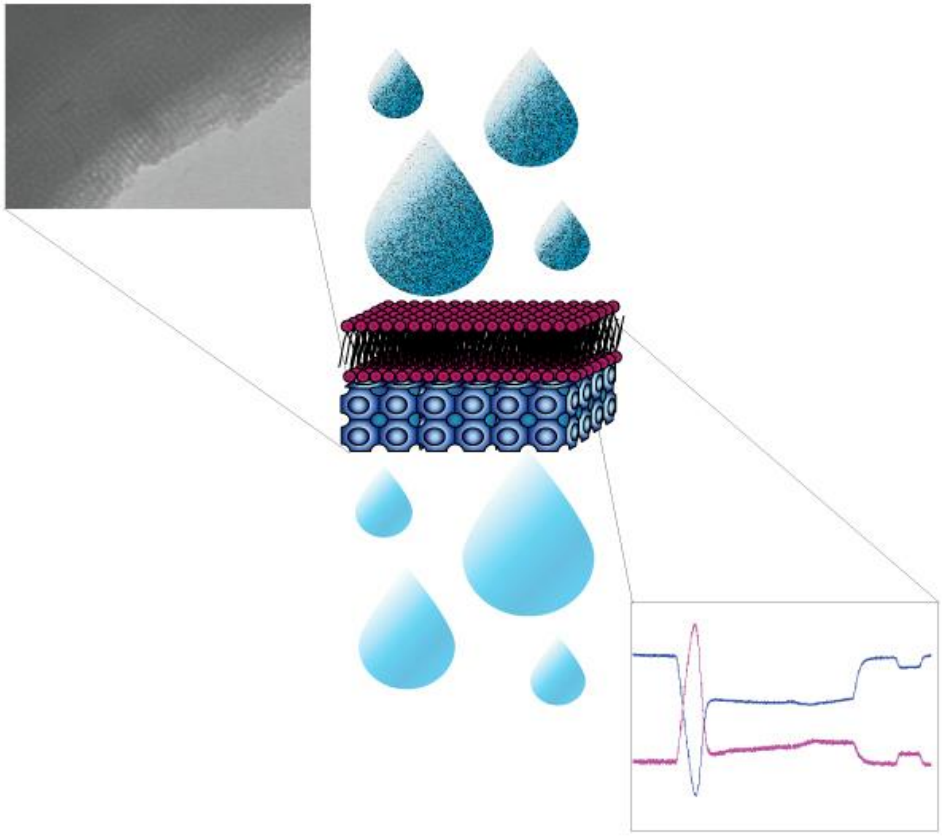

Diffusion of Water in Mesoporous Silica Thin Films Covered with Lipid Bilayers

Master of Science Thesis in the Master Degree Program, Materials Chemistry and Nanotechnology

MARIA JAPLIN

Department of Chemical and Biological Engineering
CHALMERS UNIVERSITY OF TECHNOLOGY
Gothenburg, Sweden 2014

Diffusion of Water in Mesoporous Silica Thin Films Covered with Lipid Bilayers

MARIA JAPLIN

Department of Chemical and Biological Engineering
CHALMERS UNIVERSITY OF TECHNOLOGY
Gothenburg, Sweden 2014

Diffusion of Water in Mesoporous Silica Thin Films Covered with Lipid Bilayers

MARIA JAPLIN

Department of Chemical and Biological Engineering
Chalmers University of Technology
SE-412 96 Gothenburg
Sweden
Telephone + 46 (0)31-772 1000
Supervisor: Simon Isaksson, Chalmers University of Technology
Examiner: Docent Martin Andersson, Chalmers University of Technology

Cover: Illustration depicting water treatment through a lipid bilayer supported on mesoporous silica. A TEM micrograph and a graph from QCM-D analysis can also be seen.

Gothenburg, Sweden 2014

Abstract

The access to clean drinking water is essential to life. However, there are several hundred million people that do not have access to this fundamental necessity and the need to find improved ways of water treatment is of great concern. A new possible method to clean water is by creating a lipid bilayer with proteins, aquaporins, which transport water through the lipid bilayer and let this bilayer be supported on cubic structured mesoporous silica.

In this project lipid bilayers were to be formed on mesoporous silica, both with and without aquaporins. Three pore sizes of the mesoporous silica were made using P123, BrijS10 and CTAB as templating molecules. The aim was then to study the diffusion of water in the mesoporous silica to be able to see differences in diffusion while having bilayer or not. The diffusion studies were conducted as water exchanges using QCM-D, utilising the difference in density between H_2O and D_2O. Different concentrations of D_2O in H_2O were analysed. The diffusion study was done in order to be able to provide useful knowledge about this new water treatment device.

The results from this study showed that cubic mesoporous silica with ordered regions was successfully made using the three different templating molecules. Characterisation of the mesoporous silica was made using TEM, SEM and SAXS. From the QCM-D results it was seen that lipid bilayers were able to form on both mesoporous and non-porous surfaces, both when using pure lipids and with aquaporins. It was found that having a mesoporous surface on a QCM-D crystal definitely has a huge impact on the results of the diffusion studies and that the kinetics of the water exchanges was seen to change drastically and show different behaviours in respect to D_2O concentration. It was also noticed that the ordering and the accessibility of pores also have a major impact on the results. From DLS it was determined that the proteoliposomes were bigger than the liposomes.

Keywords: mesoporous silica, lipid bilayer, water treatment, QCM-D

Acknowledgements

I would first of all like to thank my supervisor Simon Isaksson for all the help and support with everything during my thesis work, from all the laboratory work to all the battles with MATLAB. I would also like to thank my examiner Martin Andersson for all the discussions that we have had during the Thursday meetings.

I would like to acknowledge Emma Westas for the help regarding the laboratory equipment, Alexander Idström for installing different programs on the computer and Maria Wallin for the help when discussing results.

My family deserves a big thank you for keeping up with not seeing me that much during these five years I have studied at Chalmers and of course my wonderful boyfriend Viktor who is always there for me.

Last but certainly not least I would like to acknowledge the other diploma workers and project assistants in the office for all the fun activities, fikas, lunches and laughs we have shared and for the welcoming feeling that always fills the office.

Table of Contents

1 Introduction

The means to find ways to provide clean water is one of the greatest concerns in the world since there are approximately 780 million people that do not have access to an improved source of drinking water[5]. An interesting way to cope with this problem is by using biomimicry i.e. to copy nature. Think of how different trees and plants can cleanse water even in cases of contaminated water or water having a high amount of salt such as sea water. By copying nature there might be ways to facilitate easier and more energy effective ways to provide clean water.

In this project studies on a new kind of water treatment device made of a lipid bilayer supported on a cubic mesoporous silica film are to be conducted. To make the lipid bilayer more permeable to water so called aquaporins, which are water transporting proteins that can be found naturally in biological membranes[3,6-8], are incorporated in the bilayer. The resulting lipid bilayer then has a high selectivity for water and thereby is impermeable for ions and other unwanted compounds.

1.1 Background

Supported lipid bilayers have been found to be promising in many different applications and areas such as biosensors[9-12] and can also act as representations for biological cell and tissue surfaces[4,11,12]. Supported lipid bilayers are also used for water purification[6,13], but there is a need to make these more efficient and more selective regarding what substances that are allowed to pass through the membranes. One way that has been previously examined to manage this problem is to use aquaporins. Aquaporins have been found to have an extremely good selectivity when it comes to water and therefore has great potential to work as the major water permeability factor for these water treatment devices[3,6-8,13]. A study performed by Kaufman et al. showed that supported lipid bilayers containing aquaporins had far better selectivity and permeability than other devices used for water purification today that are based on the reversed osmosis technique[13].

In this study a mesoporous silica film is used as support for the lipid bilayer. The lipid bilayer is made of 1-palmitoyl-2-oleoyl-*sn*-glycero-3-phosphocholine (POPC) lipids whose interaction with the mesoporous silica has previously been studied by Claesson et al[14]. In that article they managed to successfully create lipid bilayers of POPC on mesoporous silica thin films. There are other methods to assembly supported lipid bilayers though, such as using solid supports or aperture spanning setups[4] (Figure 1). However, according to Claesson et al.

mesoporous silica is suggested to have better properties due to that it provides both sufficient support to the lipid bilayer, which is a problem with the aperture spanning support, and relieve steric constraints that can appear with solid supports which do not contain pores[4] (Figure 1).

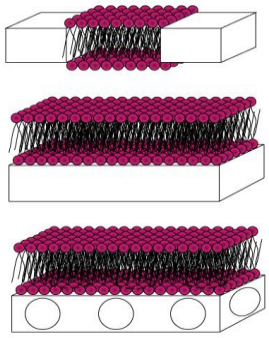

Figure 1 – Illustration of lipid bilayer supported on aperture spanning support (uppermost picture), solid support (middle picture) and mesoporous support (bottommost picture).

In this project mesoporous silica with three different pore sizes were investigated and the pore size was determined by the polymer and surfactants, also known as template molecules, used during the synthesis of the mesoporous films. The template molecules used in this project were poly(ethylene glycol)-block-poly(propylene glycol)-block-poly(ethylene glycol) (P123), polyoxyethylene(10)stearyl ether (BrijS10) and hexadecyltrimethylammonium bromide (CTAB) which are all commonly used templating agents. All the template molecules and the syntheses that have been performed with them have previously been shown to result in nicely ordered cubic mesoporous silica films[4,15-17]. The structures of the three template molecules can be seen in Figure 2.

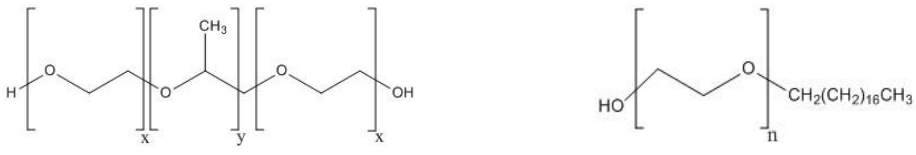

P123 BrijS10

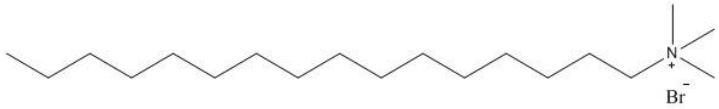

CTAB

Figure 2 – Molecular structure of the three template molecules; P123, BrijS10 and CTAB.

According to the above mentioned advantages with lipid bilayers and aquaporins on a mesoporous silica support it is believed that these elements together have the potential to be suitable for water purification.

1.2 Purpose

The purpose of this thesis was to investigate the diffusion of water in the mesoporous silica thin films covered with and without lipid bilayer and the aim was to provide helpful knowledge in this new potential way of tackling the need for clean water. The diffusion studies were performed as water exchanges with H_2O and D_2O utilising quartz crystal microbalance with dissipation monitoring (QCM-D). Questions regarding how the water diffuses through the water treatment membrane and the permeability properties of the lipid bilayer were investigated. Also, investigations were performed to see how the pore size of the mesoporous support layer effects the diffusion of water and the characteristics of the lipid bilayer. Other techniques used to investigate the different parts of the water treatment device were dynamic light scattering, transmission electron microscopy, scanning electron microscopy and small angle X-ray scattering.

1.3 Scope

This study was conducted on a very small scale, which can hopefully give some interesting new findings that can help facilitate larger scale experiments on the subject.

2 Theory

This section covers the theory behind the different concepts in this study. The different analysis methods used will also be described.

2.1 Mesoporous silica thin films

Mesoporous films are films that have a porous structure in which the pore diameters are between 2-50 nm[18]. The films can be made by a so called Evaporation Induced Self-Assembly (EISA) method where the evaporation of a solvent is the driving force for the self-assembly of templating molecules[18-20]. In this project P123, BrijS10 and CTAB were used as templating molecules and they form different kinds of structures (cubic, hexagonal or lamellar) (Figure 3) depending on pH, temperature, alcohol concentration, templating molecule/Si molar ratio and aging time[15-17,20,21]. The size of the templating molecule determines the size of the pores in the resulting film. By using the polymer P123 and the surfactants BrijS10 and CTAB the pores of the films can be tailored to specific sizes; ~6nm, ~4nm and ~2nm respectively[2,4,15-17].

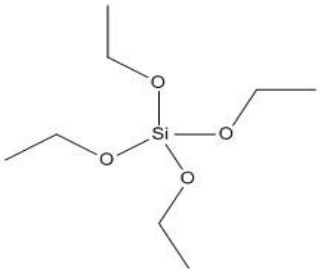

Figure 4 – Molecular structure of tetraethyl orthosilicate (TEOS).

In the production of the mesoporous films a solution containing solvent and templating molecules is needed. This solution also contains a silica precursor. The silica precursor used in this project was tetraethyl orthosilicate (TEOS) (Figure 4). When the solvent, ethanol in this case, evaporates the templating molecules order themselves. This ordering of the templating molecules also indirectly orders the silica precursors forming a silica network. The template is then removed by calcination leaving a porous structure only consisting of a silica network which results in a mesoporous silica film[15-18]. The EISA procedure is illustrated in Figure 5.

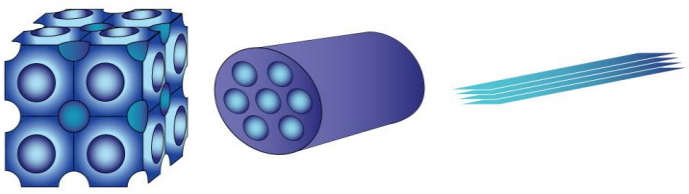

Figure 3 – Illustration showing cubic, hexagonal and lamellar mesoporous structure.

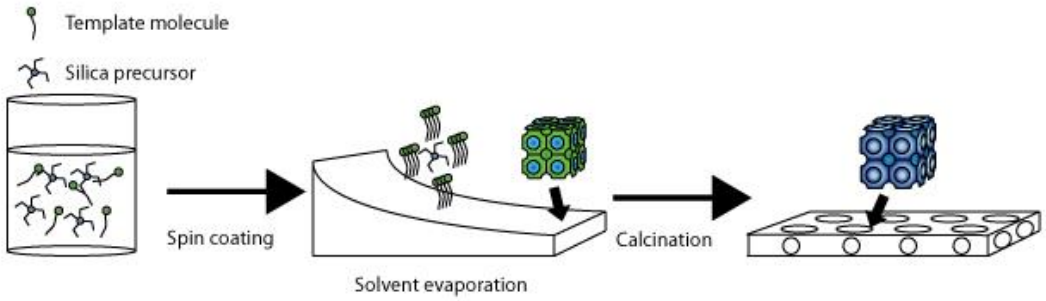

Figure 5 – A schematic picture of the EISA method starting with a mixture of solvent, template molecules, HCl and silica precursor followed by spin coating, solvent evaporation and calcination. Redrawn from Wallin; Formation of Mesoporous Materials and their use as Lipid Bilayer Supports[2].

To produce the silica network the silica precursor has to go through a hydrolysis reaction and two condensation reactions (eq 1-3) [22]. To catalyse the reaction hydrochloric acid is added to the water.

$$\equiv Si - OR + H_2O \leftrightarrow \equiv Si - OH + ROH \quad (1)$$

$$\equiv Si - OR + HO - Si \leftrightarrow \equiv Si - O - Si + H_2O \quad (2)$$

$$\equiv Si - OH + HO - Si \equiv \leftrightarrow \equiv Si - O - Si \equiv + H_2O \quad (3)$$

The structure wanted for the mesoporous silica films is a cubic structure since the pores in such a structure are bicontinuously connected to each other ensuring that the porous network is accessible from the surface, which they are not in a hexagonal or lamellar structure.

2.2 Lipid bilayers

Many lipids are amphiphilic molecules that consist of two hydrophobic chains connected to a hydrophilic head group[18]. The structure makes the lipids easy to assemble into different kinds of structures due to that they have both a part that likes water and one that does not. Depending on the concentration of lipids in a solution they assemble into different structures such as micelles or bilayers. When the lipid concentration is high enough in an aqueous solution it reaches a critical micelle concentration, CMC, and micelles starts to form[18]. When adding more lipids to the solution other structures can be formed, such as lipid bilayers.

The lipid used in this project is POPC (Figure 6), which is a phospholipid. Phospholipids are the main constituent of cell membranes[23] and when lipids are assembling into a spherical structure consisting of a lipid bilayer they are called liposomes.

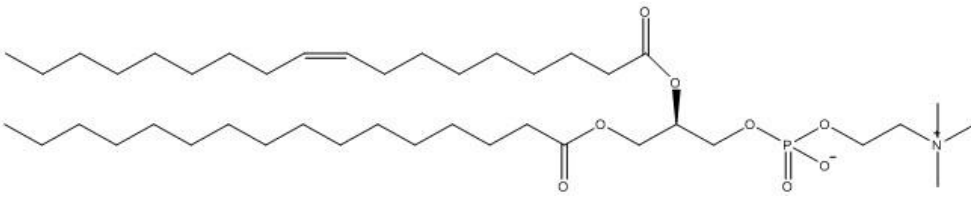

Figure 6 – Molecular structure of the lipid used in this project; 1-palmitoyl-2-oleoyl-sn-glycero-3-phosphocholine (POPC).

2.3 Aquaporins

Aquaporins are a group of membrane proteins that are found in most biological matter, both animals and plants[3,7,8]. The proteins are often situated at tissues where a lot of fluid transport is needed since they are transporters of water, but they can also transport other solutes such as glycerol. There are several kinds of aquaporins, but in this project aquaporin 4 is used which is only permeable to water. The structure of aquaporins is quite complex. They consist of 4 monomer units which are connected, where each monomer is made up of 6 α-helices creating a pore in between them (see Figure 7).

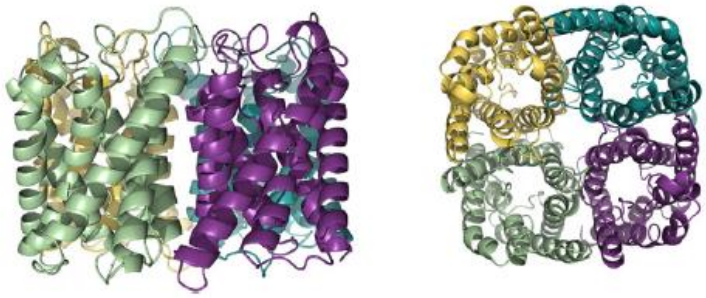

Figure 7 – Structure of aquaporins. They consist of 4 monomers, here illustrated in yellow, green, blue and purple, which are each made of 6 α-helices. Picture is taken form Tang et.al.; Desalination by biomimetic aquaporin membranes: Review of status and prospects[3].

Aquaporins reconstituted into liposomes will be referred to as proteoliposomes later in the report.

2.4 Quartz crystal microbalance with dissipation monitoring

Quartz crystal microbalance with dissipation monitoring (QCM-D) is a technique used for analysis of interaction, adsorption and viscoelastic properties of thin films in real time[24,25]. Thin films which are coated on quartz crystals are examined by oscillating the crystals with certain frequencies. Each type of crystal has its fundamental frequency, but with QCM-D so called overtones are measured as well. The overtones correspond to different frequencies: the first for 5 MHz, the third for 15 MHz, the fifth for 25 MHz and so on. By letting a liquid, for

instance water, pass the sensing side of the crystal the amount of liquid that adsorbs on and absorbs in the film can be measured. The amount of liquid that absorbs depends on the structure and composition of the thin film. The resulting mass change, due to that molecules attach to the surface of the film, is related to a change in frequency which can be described by Sauerbrey's equation[22,23] (eq 4) provided that the film is rigid. In the equation C is a constant of value 17.7 $ngHz^{-1}cm^{-2}$ for the crystals used in this project, n is the number of the frequency overtone, Δf (Hz) is the change in frequency and Δm ($ngcm^{-2}$) is the change in mass[25].

$$\Delta m = \frac{-C \times \Delta f}{n} \quad (4)$$

Dissipation gives information about the rigidity of the species adsorbing on the surface and is attained when the voltage that is causing the oscillation of the QCM-D crystal is turned off[25]. Depending on the viscoelastic nature of the film the dissipation values vary depending on how readily the energy from the oscillation is dissipating from the system[25]. For soft films, the energy is dissipating faster than for rigid films due to the viscoelastic properties of the softer film. Soft films are therefore said to be highly dissipative. The definition of dissipation is found in eq 5 where D is the dissipation, E_{Lost} is the energy lost during one oscillating cycle and E_{Stored} is the total energy stored in the oscillating sensor[25].

$$D = \frac{E_{Lost}}{2\pi E_{Stored}} \quad (5)$$

A standard QCM-D crystal has a diameter of 14 mm, but the active sensor area of the crystal is not homogenously distributed over the whole surface of the crystal[1,26]. The sensing area therefore needs to be considered while investigating the QCM-D results after analysis. During the experiments conducted in this thesis, the third overtone (15 MHz) has been analysed, which gives a sensing radius of the crystal of ~4mm from the middle of the crystal (Figure 8).

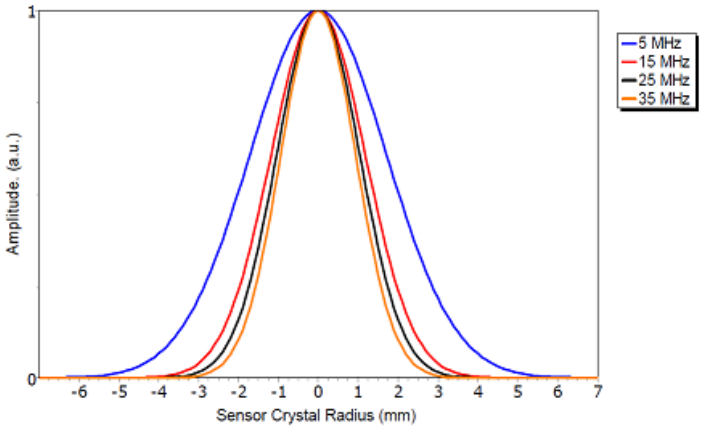

Figure 8 – Illustration showing the active sensor radius of a QCM-D crystal depending on overtone. Figure is taken from http://www.q-sense.com/support-education/faq-qcm-d/the-qcm-d-principle[1].

For this thesis QCM-D is used to get information about the diffusion properties of water inside the mesoporous silica network with and without lipid bilayer. In previous studies lipid bilayers have been studied with QCM-D and it has been shown that a lipid bilayer result in a frequency change of ~-26 Hz and that the resulting change in dissipation should be small[14,27]. Figure 9 is showing what is happening during lipid bilayer formation from when the vesicles, in this project known as liposomes or proteoliposomes, attach to the surface until they eventually rupture.

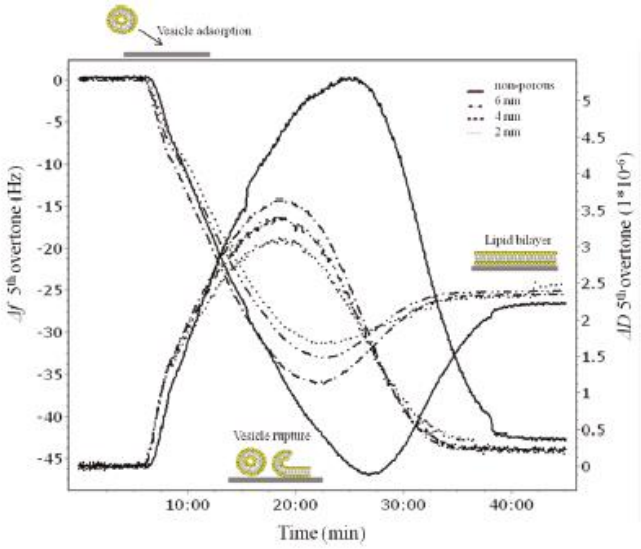

Figure 9 – Graph showing the change in frequency and dissipation during the different stages of lipid bilayer formation; vesicle adsorption, vesicle rupture and lipid bilayer creation. Figure is taken from Claesson et. al.; Pore Spanning Lipid Bilayers on Mesoporous Silica Having Varying Pore Size[4].

2.5 Transmission electron microscopy

Transmission electron microscopy (TEM) is a characterization method that uses an electron beam to irradiate a sample[27]. The electron beam is emitted from an electron gun which passes through a set-up of condenser-lenses before hitting the sample. When the electrons reach the sample the electrons interact with it while passing through it. Therefore, samples prepared for TEM must be very thin to enable the passing of the electrons[27]. The electrons that pass through the sample are detected and produce an electron density map of the sample. X-rays caused by the electrons hitting the sample can also be analysed[27]. TEM samples of metals and some other materials can be used directly as small discs, but this is not possible for all kinds of samples. These samples must be transferred to a copper grid. The samples for this project have to be placed on such copper grids and the purpose for using TEM in this project is to characterize the mesoporous silica films. By using TEM it is possible to visualise the porous structure and to be able to get an approximate value of the size of the pores that ought to be present in the films.

2.6 Scanning electron microscopy

Scanning electron microscopy (SEM) is a characterisation method where an electron beam is focused at a sample and an image can be obtained[28]. Unlike TEM, SEM samples do not need to be thin since the electrons do not need to pass through the sample, making SEM a bulk characterisation method[28]. What can be detected with this method are the secondary electrons, back scattered electrons, Auger electrons or X-rays emitted from the sample[28]. SEM is performed in this project to get a measurement of the thickness of the mesoporous silica films.

2.7 Small angle X-Ray scattering

Small angle X-ray scattering (SAXS) is an important characterisation method when looking at ordered materials[18], in this case ordered mesoporous silica. An X-ray beam is passing through a sample and the scattered X-rays are detected. Depending on the ordering of the sample structure the X-rays scatter differently and give certain patterns, called diffraction patterns[18]. From these patterns it is possible to get information about how and if a sample is ordered. For example a cubic structure should have peaks at the intervals 1, $\sqrt{2}$, $\sqrt{3}$, 2, $\sqrt{5}$. The diffraction is dependent on several factors which can be related to each other by Bragg's law (eq 6). In Bragg's law λ is the wavelength of the incoming beam, θ is the angle of the incoming beam, d is the distance between the lattice planes in the sample structure and n is an integer[18].

$$n\lambda = 2d * sin\theta \ (6)$$

2.8 Dynamic light scattering

Dynamic light scattering or DLS is a method to characterise the dimensions of nano sized particles in solution[29]. By aiming a laser through the sample the fluctuations in intensity of the scattered light can be detected. The fluctuation in intensity is caused by the velocity of the Brownian motion of the particles and therefore the fluctuations can therefore be said to depend on the size of the particles, since e.g. larger particles have a lower velocity then smaller ones[29].

DLS is used in this project to estimate the size of the POPC liposomes, with and without aquaporins, which are used for the lipid bilayer.

3 Materials and methods

In this section the preparation of the water treatment device components are described. The equipment and chemicals used are also presented. All experiments were conducted at room temperature. All abbreviations that are used throughout the report can be found in this section.

3.1 Chemicals and substrates

Poly(ethylene glycol)-block-poly(propylene glycol)-block-poly(ethylene glycol) (P123) (Aldrich), polyoxyethylene(10)stearyl ether (BrijS10) (Aldrich) and hexadecyltrimethylammonium bromide (CTAB) (≥ 98%, Sigma) were used as template compounds in the synthesis of the mesoporous silica thin films. Tetraethyl orthosilicate (TEOS) (Reagent grade, 98%, Aldrich) was used as the silica precursor. The water used for the experiments was of milli-Q quality (18.2 MΩ.cm 25°C, Millipore) and the ethanol used for the syntheses was Solveco Etanol 99.5% (EtOH) (Solveco AB). Hydrochloric acid (HCl) (37%, Sigma-Aldrich) was also used for the syntheses of the mesoporous thin films. The glass slides used as substrates for the films were microscope slides (VWR International LLC) and the QCM-D crystals (Q-Sense AB) used, also called QCM-D sensors, where coated with silica. Sodium dodecyl sulphate (SDS) (Sigma-Aldrich) was used for washing the substrates. The lipid used for making the lipid bilayer was 1-palmitoyl-2-oleoyl-*sn*-glycero-3-phosphocholin (POPC). In the buffer used for the lipids, sodium chloride (NaCl) (ReagentPlus®, ≥ 99.5%, Sigma-Aldrich) and tris(hydroxymethyl)aminomethane (Tris) (ACS reagent, >=99.8%, Sigma-Aldrich) was used. Deuterium oxide (D_2O) (99.9 atom % D, Sigma-Aldrich) was used for the water exchanges performed during QCM-D analysis. The aquaporins used were kindly provided from Kristina Hedfalk at the division of Biochemistry and Biophysics at the department of Chemistry and Molecular Biology at Gothenburg's University.

3.2 Machines and programs

The machine used for sonication was an Ultrasonic cleaner (VWR International LLC). The spin coater used for making mesoporous silica films was a Spin150-v3 (SPS-Europe) and the ovens used for calcination were of model L3 from Wilhelm Tham AB and Nabertherm GmbH. The QCM-D equipment (Q-Sense AB, Gothenburg, Sweden) consisted of a Q-Sense E4 system which contained a QE 401 electronics unit, a QCP 401 chamber platform, a QFM 401 flow module and the software QSoft 401. The transmission electron microscope (TEM) used was a JEM-1200 EX II TEM (JEOL, Tokyo, Japan) and the grids used for TEM analysis

were of Lacey Formvar/Carbon 300 mesh type (Ted Pella Inc). The device used for pH measurements was a laboratory pH meter, model 827 pH lab, from Metrohm and the device was calibrated before each use. The small angle X-ray scattering was performed at MAX IV Laboratory in Lund at the I911-4 beamline [30]. The devise used for the dynamic light scattering (DLS) was a Zetasizer Nano ZS (Malvern Instruments Ltd, Worcestershire, UK) and the cuvettes were of UVette model (Eppendorf). The scanning electron microscope (SEM) used was a Leo Ultra 55 FEG SEM (Leo Electron Microscopy, Cambridge, UK).

The computer program used while analysing the QCM-D results was MATLAB and for measuring pore sizes and film thicknesses from TEM and SEM samples the program ImageJ was used.

3.3 Preparation of solutions

Solutions of HCl and milli-Q water were prepared, one with pH 2 (0.01 M HCl) and one with pH 1.25 (0.056 M HCl). Two glass bottles were filled with milli-Q water and were stirred at 300 rpm while pH was measured. HCl was added to the bottles dropwise until the pH reached 2 and 1.25 respectively.

A Tris buffer was used for the liposomes and proteoliposomes. It consisted of milli-Q water with 50mM NaCl and 50mM Tris. The pH was then corrected to pH 8 by adding HCl dropwise to the solution under stirring and constant measuring of the pH.

3.4 Washing of substrates

Both glass slides and QCM-D crystals were used as substrates for mesoporous silica films. The glass slides were used as substrates for films made for TEM, SEM and SAXS analysis and the QCM-D crystals were used for QCM-D analysis. The substrates where washed in a 2 wt-% SDS solution, milli-Q water and EtOH (99.5%). The substrates were sonicated for 2 minutes at maximum frequency in each liquid. When the sonication was done the substrates were dried using nitrogen gas.

3.5 Synthesis of mesoporous silica thin films

Three different syntheses were performed to provide three different pore sizes of the mesoporous silica thin films. The syntheses are based on syntheses previously performed by Alberius et al[15], Coquil et al [17] and Besson et al[16].

3.5.1 P123

2g of EtOH and 1.73g TEOS was added to a vial and was left stirring for ~1 minute on a magnetic stirrer plate at 150 rpm. 0.9g HCl (0.01 M) was added dropwise to the solution and was left stirring for 20 minutes at 150 rpm. After 20 minutes 0.28g P123 dissolved in 1.33g EtOH was added dropwise to the TEOS solution using a Pasteur pipette. The resulting solution was left to stir at 300rpm for another 20 minutes before spin coating was performed.

3.5.2 BrijS10

0.8g of EtOH and 1.0g TEOS was added to a vial and was left stirring for ~1 minute on a magnetic stirrer plate at 150 rpm. 0.1g HCl (0.01 M) was added dropwise to the solution and it was left stirring for 20 minutes at 150 rpm. After 20 minutes 0.17g BrijS10 dissolved in a solution of 3.6g of EtOH and 0.34g HCl (0.01 M) was added dropwise to the TEOS solution using a Pasteur pipette. The resulting solution was left to stir at 300rpm for another 30 minutes before spin coating was performed.

3.5.3 CTAB

0.365g of EtOH and 0.445g of TEOS was added to a vial and was left stirring for ~1 minute on a magnetic stirrer plate at 150 rpm. 0.19g of HCl (0.056 M) was added dropwise to the solution and it was left to stir at 170 rpm in a water bath, 40°C, for 2 hours. After 2 hours a solution of 0.089g of CTAB dissolved in 2mL of EtOH was added to the TEOS solution. The resulting solution was left to stir for another 15 minutes in the 40°C water bath before spin coating was performed.

3.5.4 Spin coating and aging

A clean substrate, glass slide or QCM-D crystal, was put in the spin coater and was held in place by vacuum. The spin coater was allowed to come up to 4000 rpm before solution was added to the substrate. On glass slides 5-7 droplets of solution were dropped on the slide using a Pasteur pipette and on QCM-D crystals 30µL of solution was added using an Eppendorf pipette. The spin coater was run for 60 seconds. The coated substrates were allowed to age in room temperature for approximately 24 hours and were then put in an oven for calcination. The oven temperature was brought from room temperature to 400°C (1°C/minute) before the temperature was held constant at 400°C for four hours.

3.6 TEM analysis

The thin films spin coated on glass slides for TEM analysis were scraped off using another clean glass slide. Thin films from 1-2 glass slides were used for each TEM sample. The resulting powder of thin film was collected and transferred to a small vial. EtOH was added dropwise into the vial until an adequate concentration of the scraped thin film was reached. The concentration was verified visually. The solution was then sonicated for 2 minutes at maximum frequency. After sonication 3 droplets of the solution were dropped on a prepared TEM grid. The EtOH was allowed to evaporate for 10-15 minutes. The TEM samples were analysed at 120 kV.

3.7 SAXS analysis

The samples for the SAXS analysis were made from thin films that had been scraped from glass slides the same way as with the TEM samples. The resulting powder was then placed on a piece of kapton tape covered with another piece of the same tape to encapsulate the powder. The sample was then placed in a sample holder before the SAXS measurement was performed. The measurements were carried out for 120 seconds per sample. A reference sample with only kapton tape was also made and used for background subtraction.

3.8 QCM-D analysis

QCM-D analyses were performed on both spin coated QCM-D crystals and a non-coated reference crystal. The QCM-D machine has 4 chambers, so four crystals were analysed at a time and a flow of 50µL/minute was used during all the QCM-D analyses. The analyses were performed as H_2O and D_2O exchanges where pure milli-Q water was changed to different concentrations of D_2O. The concentrations of D_2O used were 5, 40, 60 and 99.9 wt-% in milli-Q water. This was done to get a measurement of how the different mesoporous surfaces interact with the milli-Q water compared to heavy water. These experiments were performed on both clean mesoporous and non-porous QCM-D crystals as well as on crystals where lipid bilayers had been formed.

To create a lipid bilayer during QCM-D analysis a baseline with milli-Q was first established. After that Tris buffer followed by a solution containing liposomes was let to flow over the crystals. After a potential lipid bilayer was created Tris buffer was again added. The Tris buffer was then changed to milli-Q water and H_2O and D_2O exchange was performed. Lipid bilayers containing aquaporins were also attempted to be formed, so the liposome solution was in these cases changed to a solution containing proteoliposomes.

2 runs with 2 QCM-D crystals with the same mesoporous surface were run and 4 exchanges of each D_2O concentration was made each time during the experiments without liposomes used. For half of the water exchanges the D_2O sample was sonicated before analysis.

The same QCM-D crystals were used for trying to create lipid bilayers so that the results would be easy to compare. For the experiments involving liposomes or proteoliposomes only 2 water exchanges were conducted during each experiment.

The same non-porous reference crystal was used during all experiments. The data obtained from the QCM-D measurements was presented as graphs which were analysed using MATLAB to get valuable information about the different diffusion behaviours of the different surfaces.

3.9 DLS analysis

Solutions containing Tris buffer with liposomes and proteoliposomes respectively were measured using DLS. The samples were measured at a concentration of 0.025 mg/mL and were diluted with Tris buffer.

3.10 SEM analysis

For the SEM analysis spin coated glass slides with mesoporous silica was cut in half with a glass cutter. The cut surface was then analysed. The SEM analysis was conducted at 5 kV.

4 Results

Here the results from the different analytical methods TEM, SEM, SAXS, QCM-D and DLS are presented. The results contain information about the structure of the mesoporous silica and diffusion properties of water inside it with and without lipid bilayer as well as the size of the liposomes and proteoliposomes. In this part of the report all the mesoporous samples will be named after the templating molecule used to make them.

4.1 Characterisation of mesoporous silica

The results from the TEM analyses can be seen in Figure 10 and indicate that regions of nicely ordered cubic structure were found in all the different kinds of mesoporous silica. An image from SEM can also be seen in Figure 10. The pore sizes measured from the TEM micrographs and the thickness of the films measured from SEM images can be found in Table 1 and shows that P123 has the biggest pores and also produce the thickest films. When CTAB was used as templating molecule the smallest pores were produced and the film was thinner than for the P123 sample.

Table 1 – Table showing results from the measured film thicknesses and pore sizes gained from the different templating agents

Templating agent	Pore size	Film thickness
P123	6-7 nm	290 nm
BrijS10	3-4 nm	
CTAB	1.5-2 nm	220 nm

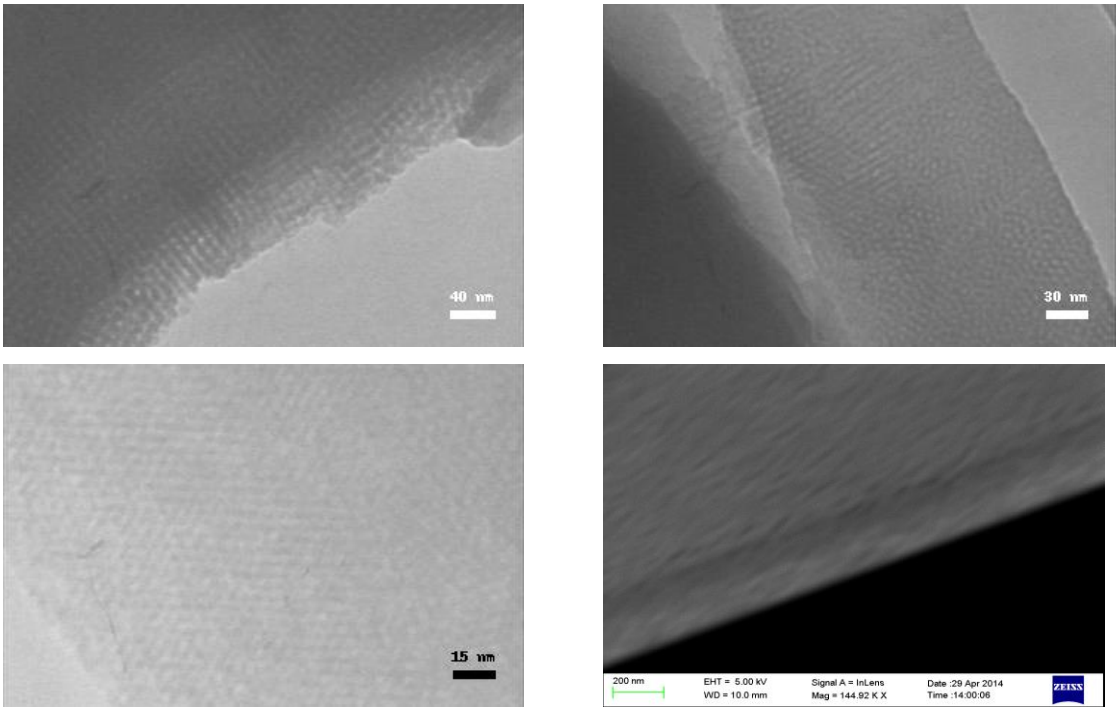

Figure 10 – TEM micrographs of the ordered mesoporous silica: P123 (uppermost picture on the left), BrijS10 (uppermost picture on the right) and CTAB (bottommost picture to the left). The bottommost right picture is an image from SEM showing a cross section of a mesoporous thin film.

BrijS10 had the second largest pores, but no film thickness could unfortunately be obtained from the BrijS10 sample. However, during sample preparation for TEM and SAXS it was noticed that less material was obtained from the BrijS10 samples compared to P123 and CTAB, which might indicate that the BrijS10 samples were the least thick.

From the SAXS measurements, see Figure 11, the results suggest that both the P123 and the CTAB samples are of a cubic structure since the peaks seem to fit the cubic peak pattern where the peaks are situated at certain q-value intervals; 1, √2, √3, 2, √5. Lamellar and hexagonal structures should not show peaks at these positions. The results from the BrijS10 samples are hard to interpret since no distinct peaks can be observed. However, a tendency to a peak can be seen, which is marked for the BrijS10 sample in Figure 11. The peaks from the three kinds of samples where all found at different q-values. The CTAB peaks were at the highest q-value followed by BrijS10 and P123. The peaks appearing at q-value ~4 was due to the kapton tape used for holding the sample.

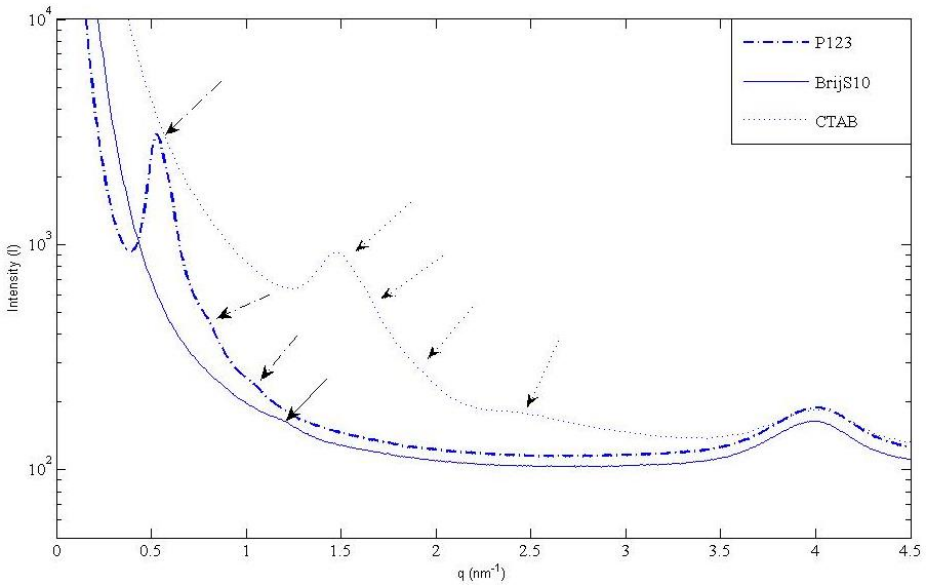

Figure 11 – SAXS results of mesoporous silica films made with P123, BrijS10 and CTAB as templating agents. The arrows in the figure are pointing towards peaks. The peak at q-value 4 corresponds to kapton.

4.2 QCM-D measurements

The results from the H_2O and D_2O exchange resulted in a drop in frequency due to that D_2O is heavier than H_2O. This drop was then analysed by measuring the change in frequency, the slope of the curves going down and up and also by fitting an exponential model to the curves where the exchange takes place. These areas of interest can be seen in Figure 12. The curves

where analysed by using MATLAB. The analysed frequency change could then also be translated into change in mass using eq 4 to get a value of the volume of D_2O in a sample. The slope was measured to see if there was any difference in kinetics while going from H_2O to D_2O or going from D_2O to H_2O. For the same reason the exponential fitting was done. By fitting an exponential model to the two areas that are marked green in Figure 12 a value of the speed of the exchange is gained, here called a b-value. When changing from H_2O to D_2O the curve was fitted to the model $a * e^{-bx} + c$ and for D_2O to H_2O the exponential model $c - a * e^{-bx}$ was used. All the analysis data for all the measurements are found in Appendix A.

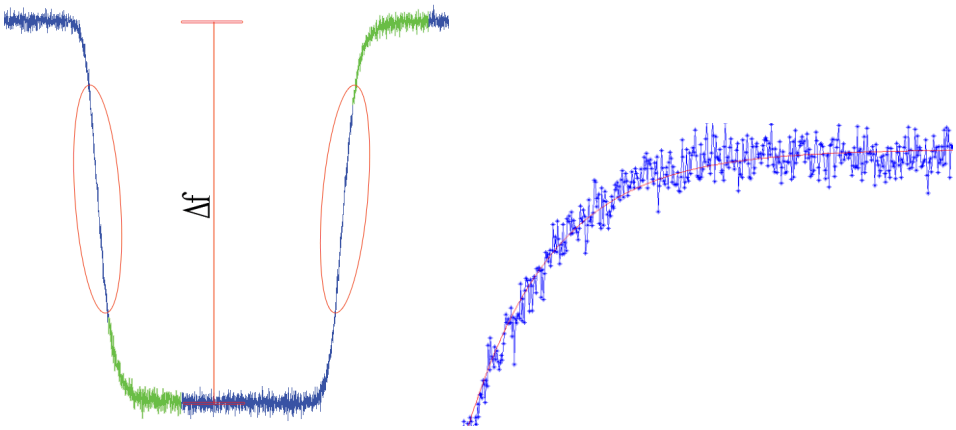

Figure 12 – Left image: Representative graph showing change in frequency during H_2O and D_2O exchange (blue curve) with marked areas of analysis (red and green). Right image: Close up of how a curve fitting looks like. The blue points are the data points that are being analysed and the red curve is the fitted exponential curve.

4.2.1 H_2O and D_2O exchange on mesoporous silica

In Figure 13 the results from the H_2O and D_2O exchange on the mesoporous and non-porous surfaces can be seen. It is seen that P123 results in the largest change in frequency followed by CTAB, BrijS10 and the non-porous reference. In both runs this was the outcome. However, when comparing the two runs one of the BrijS10 samples had a higher frequency change than the CTAB sample from the other run which can be seen in Figure 14. When looking at the TEM micrographs of the BrijS10 sample that got the lowest result no pores were found.

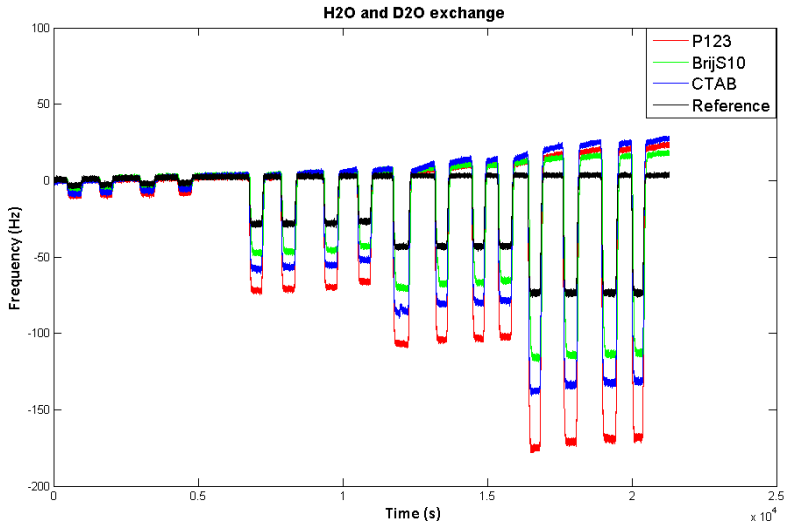

Figure 13 – Representative graph showing the frequency change resulting from D_2O and H_2O exchange. Non-porous reference is shown in black, mesoporous silica made from templating molecule P123 is seen in red, CTAB in blue and BrijS10 in green.

While analysing the QCM-D graphs closer it was found that the values of the slopes while exchanging liquids followed the same pattern as the change in frequency i.e. it went faster for P123 and slowest for the reference both when changing from H_2O to D_2O as well as when changing from D_2O to H_2O. When looking at how the concentration of D_2O influenced the results a linear behaviour was found in how the frequency and the slope changed. The higher the concentration the faster the exchange goes and the larger the frequency change. When locking at exchange with pure D_2O the slope was generally steeper for the H_2O to D_2O than for D_2O to H_2O.

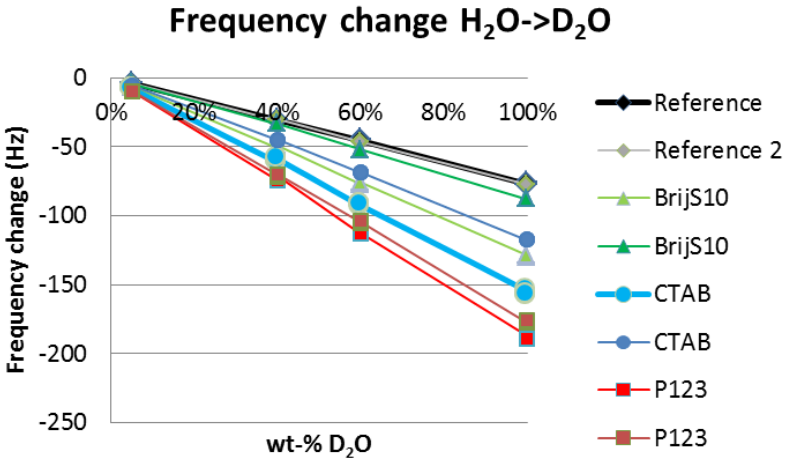

Figure 14 – Graph showing the linear behaviour of the frequency changes resulting from H_2O to D_2O exchange from QCM-D. What the different data points represent can be seen in the legend and the names represent which templating molecule that was used making the mesoporous silica and the reference is the non-porous sample.

When analysing the exponential curve fit it was seen that the concentration did not show the same linear behaviour as with the frequency change and slope values. The b-value seem to increase from the lowest concentration, reach a maximum value at 40 or 60 volume-% D_2O and then decrease for pure D_2O which can be seen in Figure 15.

No difference was observed when sonicating the D_2O samples for mixing purposes.

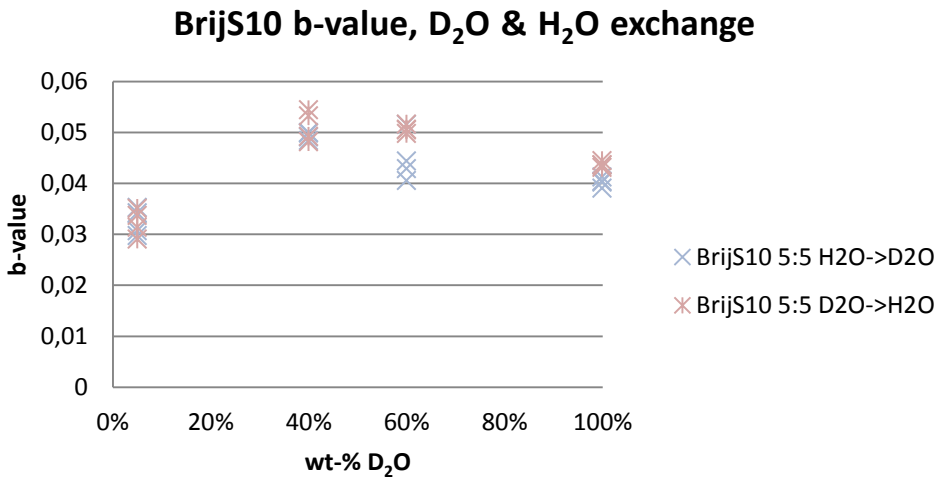

Figure 15 – Here the results from one of the mesoporous coated QCM-D crystals (BrijS10 was used as templating molecule) is shown as a representative graph displaying the behaviour of the b-value when changing concentration of D_2O.

4.2.2 Lipid bilayer formation with liposomes

Lipid bilayers formed using liposomes were created on all types of surfaces, both the mesoporous ones and the non-porous reference, which can be seen in Figure 16. In the graph it is seen that bilayers formed using P123 and BrijS10 as templating molecules shows the expected frequency change of ~-26Hz that is typical for bilayers and that the resulting dissipation change is small[14,31]. When looking at the reference sample the frequency change is a bit higher than expected and the resulting dissipation change is a bit high. For the CTAB sample the frequency change is less than for the other mesoporous samples. However, the dissipation change is as anticipated with lipid bilayer formation.

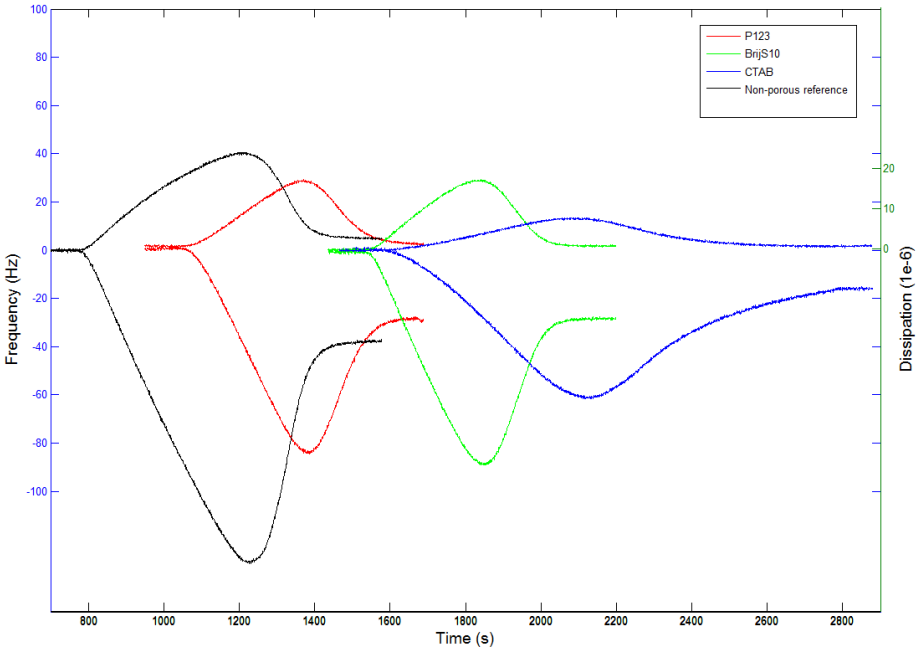

Figure 16 – Graph showing the change in frequency (bottommost curves) and dissipation (uppermost curves) during formation of lipid bilayers. Bilayer formation on non-porous reference is shown in black and the red, green and blue curve is from mesoporous silica made with P123, BrijS10 and CTAB respectively.

4.2.3 Lipid bilayer formation with proteoliposomes

The results from the formation of lipid bilayers using aquaporins reconstituted in liposomes can be seen in Figure 17. It does not show the same bilayer formation behaviour as the ones formed with liposomes. However, lipid bilayers might have been formed on some surfaces after change to H_2O occurred. As can be seen in Figure 17 the frequency goes up and the dissipation goes done at approximately 4700 seconds, which corresponds to change in fluid from the Tris buffer to milli-Q water.

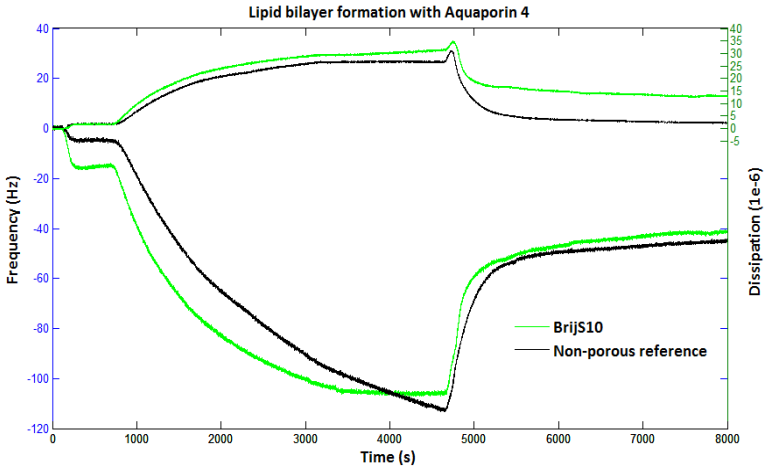

Figure 17 – Graph showing the change in frequency (bottommost curves) and dissipation (uppermost curves) during formation of lipid bilayers with proteoliposomes on one mesoporous surface, BrijS10, (green graphs) and the non-porous reference (black graphs).

4.2.4 Lipid bilayer H_2O-D_2O exchange

The results from the H_2O and D_2O exchange with bilayer made using liposomes were compared with the results gained from the same QCM-D crystal without bilayer. The results from the proteoliposomes were not compared since lipid bilayers were not able to form on all surfaces. It was found that there was a slight decrease in the frequency change when having bilayer for all samples except for the CTAB sample which shows the opposite (see Figure 18). The results did show the same trend as for the ones without bilayer with regard to that the frequency change as well as the value of the slopes were largest for P123, then CTAB, then BrijS10 and lastly the reference.

Regarding the slopes it was found that the slopes for the mesoporous structures made with P123 and BrijS10 were slightly increased when bilayer was formed when going from H_2O to D_2O. The reference sample showed the opposite and the CTAB sample showed no clear differences. When going from D_2O to H_2O the BrijS10 and CTAB samples with bilayers showed increased slope values, but for P123 and the reference the results showed no clear differences. The frequency change and the slope show the same linear behaviour as the ones without bilayers.

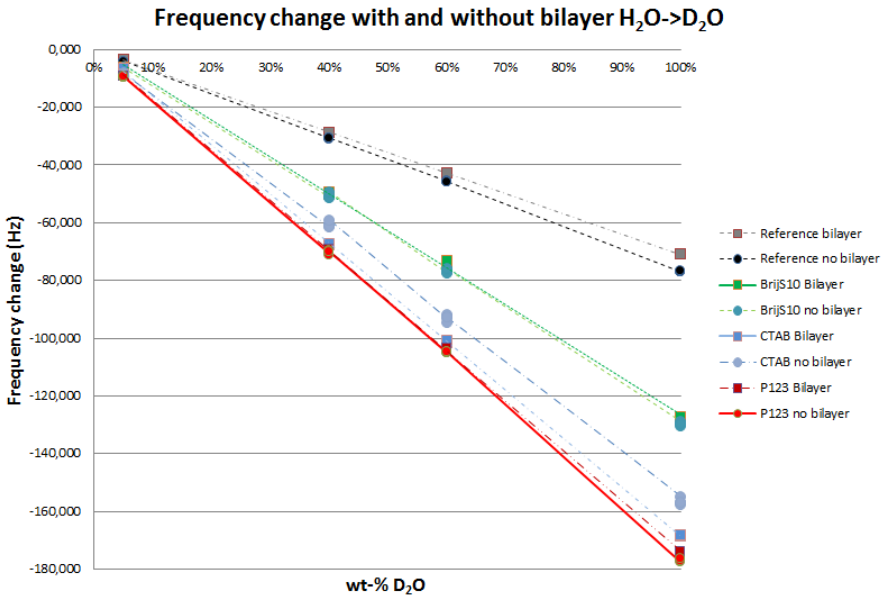

Figure 18 – Graph showing the frequency changes when having lipid bilayer or not. What the different data points represent can be seen in the legend.

When looking at the b-values from the curve fitting the reference, the P123 sample and the BrijS10 samples also showed an increase in these values when going from H_2O to D_2O. For the CTAB sample it was hard to see any clear difference. The b-values where though hard to

compare with the ones obtained from the D_2O to H_2O exchange since the curve for D_2O to H_2O did not seem to fit the exponential model used.

The results from the lipid bilayers were not compared with these results since bilayers were not formed on all the mesoporous surfaces.

4.2.5 Calculation of the accessible volume in mesoporous films

From the frequency changes measured for the H_2O and D_2O exchanges performed with pure D_2O the volume of H_2O that was accessible by the porous structure in a mesoporous thin film could be calculated. By using eq 4 the change in frequency change gained from the water exchange experiments could be translated into volume. A calculation from one of the analyses is shown below. The change in frequency for the non-porous sample was -76.363 Hz and for the mesoporous one was -176.292 Hz for this case. All other data can be found in Appendix A.

By using Sauerbrey´s equation (eq 4) the mass of H_2O can be calculated and since there is a difference in density between the liquids ($\rho_{D_2O} = 1.107 gcm^{-3}, \rho_{H_2O} = 1.00 gcm^{-3}$) this must be considered. By multiplying with the sensor area the volume of H_2O was calculated. As the third overtone was used in this project the sensing area was approximately $0.4^2\pi$ since the sensing radius is about 0.4 cm (see Figure 8).

$$V_{H_2O} = \frac{-C \times \Delta f}{n(\rho_{D_2O} - \rho_{H_2O})} \times sensing\ area = \frac{-17.7 ngHz^{-1}cm^{-2} \times \frac{(-176.292-(-76.363))Hz}{(1.107-1.00)gcm^{-3}}}{3} \times 0.4^2\pi\ cm^2 =$$

$$= 2.77 \times 10^{-6} cm^3$$

From these calculations a percentage of how much of the total film volume this corresponds to can be calculated and an assumption that the total film volume consisted of water was made. In this case the film thickness was 290 nm and the sensing area was the same as above.

$$\frac{V_{H_2O}}{V_{film}} \times 100 = \frac{2.77 \times 10^{-6} cm^3}{290 \times 10^{-7} cm \times 0.4^2 \pi cm^2} \times 100 \approx 19\%$$

For this example approximately 19% of the film was filled with water.

4.3 DLS measurements

The results from the DLS can be seen below in Figure 19. From these results it was found that the liposomes had an average size of 163.6 ±57.14 nm and the proteoliposomes had an average size of 202.5 ±62.74 nm.

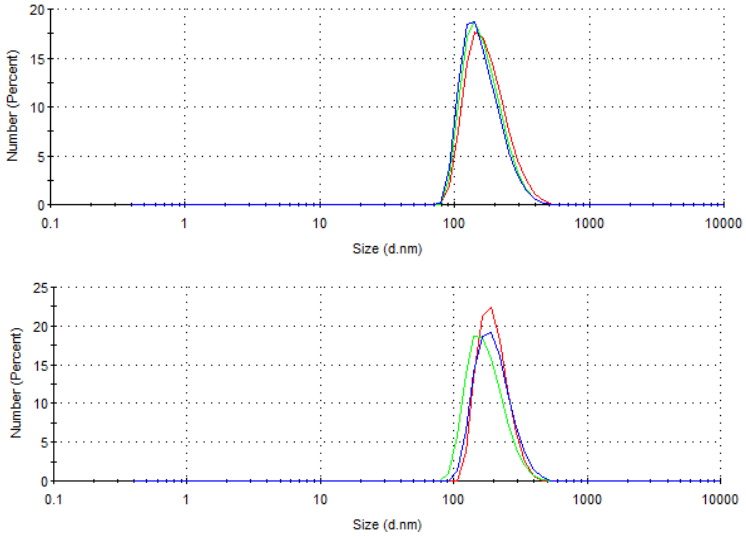

Figure 19 – Graphs from the DLS measurements of liposomes (upper graph) and proteoliposomes (bottom graph).

5 Discussion

In this section the results presented in the report will be discussed. As in the results section all the mesoporous samples will be named after the templating molecule used to make them.

5.1 Characterisation of mesoporous silica

The pore sizes measured in this report corresponds well to sizes previously reported in other studies[2,4,15-17] and the thicknesses of the films also seems to be of realistic numbers. In other studies they have also seen that P123 resulted in the thickest films and that the thickness decrease with decreasing pore size[2]. This assumption fits for CTAB as well, since the smaller pore size gave a thinner film. However, this is hard to tell if BrijS10 follows the same pattern as no value of the thickness was obtained for this sample. The observation during sample preparation for TEM and SEM was that BrijS10 gave the least amount of sample, which implies that the BrijS10 samples are thinner than CTAB. However, it is hard to know just from visual observations. The reason for not measuring the BrijS10 was that there were some problems with the SEM equipment. It should though be noted that the film thickness probably varies from batch to batch and only one sample each from P123 and CTAB were analysed.

When looking at the results obtained from the SAXS measurements it would seem that P123 and CTAB resulted in the most ordered structures. Both P123 and CTAB show peaks that correspond to a cubic phase. The most distinct CTAB peak also fits well to the cubic structure in a previous study which suggests that the cubic structure would belong to the primitive cubic structure Pm3n or $P\bar{4}3n$[16]. The result that there was only a small indication of a peak for the BrijS10 sample might suggest that the sample was not that ordered. However, this small indication of a peak does make it easier to confirm that there are indeed different pore sizes in the different samples, since the peaks show up at different q-values depending on the pore size. This corresponds well to previous studies and is believed to be due to that the centres of neighbouring pores become closer together with smaller pore sizes[4,32]. These results then confirm that P123 have the largest pores followed by BrijS10 and CTAB. When comparing these results with the ones obtained from the TEM analysis, the TEM results show nicely ordered regions of cubic structured mesoporous silica in all mesoporous samples. From TEM analysis it is assumed that BrijS10 also has a cubic structure, but it should be mentioned that a very small piece of a total sample is analysed in TEM.

5.2 QCM-D measurements

When looking at the results from the H_2O and D_2O exchange both with and without bilayers the results clearly show the effect of the porous structure. There is definitely a noticeable difference between the non-porous and the mesoporous surfaces. When looking at the differences between the mesoporous samples P123 results in the greatest frequency change as well as the highest value of the slopes. This is seen both when going from H_2O to D_2O and from D_2O to H_2O. This suggests that P123 has the largest porous volume accessible to the water followed by CTAB and BrijS10 since the greater the frequency change is the more mass is in the sample.

From the calculations done on the frequency changes they confirm the results from the experiments. For all calculations but one P123 has the most available surface area even though it is thickest and therefore has a larger factor to divide with. However, this goes against previous results gained in other studies where CTAB is calculated to have the most accessible volume for the water followed by BrijS10 and lastly P123[2,4]. It is therefore believed that the results of the frequency changes depend much on the ordering of the pores and on that there is a continuous porous structure over the surface. This theory might explain the difference in the results gained in this report and the ones from previous studies.

Other results that goes along with the theory that the ordering and presence of pores over the whole surface has a large effect on the out coming results are the ones gained from H_2O and D_2O exchange for the different BrijS10 samples, which can be seen in Figure 14. For the BrijS10 sample that showed very low values for the frequency change, almost as low as the non-porous sample, it was hard to find any pores while analysing that sample batch in TEM. As a contrast, the other BrijS10 sample resulted in a higher frequency shift, even higher than one of the CTAB ones. This further strengthens the theory that the ordering or amount of pores has a large impact on the resulting frequency change. Another thing these results show is the difficulty when it comes to replicating the films since it can be observed that QCM-D crystals with the same mesoporous structure on them can give quiet deviating results.

When looking at the change in frequency when adding a lipid bilayer a small decrease was observed, except for the CTAB sample. Why the CTAB sample shows the contrary is hard to explain, but it was seen that the bilayer formation might not be complete on this surface since the resulting frequency change after the bilayer was formed was ~-20 Hz. This indicates that only patches of bilayer were created and that perhaps this did not affect the water that much.

Regarding the lipid bilayer formation on the non-porous reference the frequency change after bilayer formation was higher than expected for bilayers, ~-35 Hz. Also the dissipation of this sample did not go down as much as for the other samples and this suggests that there were still vesicles that did not collapse left on the surface. Even though, this sample showed a lowering in the frequency change during water exchange. A change in frequency was not expected since it is believed that the lipid bilayer only gives a slower exchange of the water and therefore should not result in any difference in frequency.

Regarding the slope values from the water exchange analysis the slope going from H_2O to D_2O was generally steeper than the other way around. This means that it went faster to change to D_2O than change from D_2O to H_2O. An answer for this might be that the driving force for exchanging D_2O to H_2O might be lower. D_2O is heavier than H_2O, which might make it harder for the H_2O molecules to replace the heavier molecules. It was also seen that for some of the samples with bilayer it went faster to exchange the water than when not having a bilayer. The same effect was also seen for the b-values where the values where generally higher for the ones with bilayer. This is not an expected result as the lipid bilayer in theory is, as mentioned before, making the water exchange slower.

Looking further at the b-values they showed that there are not such a big difference in the obtained values between the mesoporous and non-porous samples. Why the b-values are not as affected as for instance the frequency change might be because these areas of analysis depend more on the liquid than the porous structure. This suggests that the larger differences in the frequency change and slope values between the different samples are more likely to be due to the porous structure.

When it comes to the different behaviours of the frequency change, the slope and the b-values it is easier to explain the linear behaviour found for the frequency change and the slope. As the concentration of D_2O increases the more mass end up in the pores and therefore a larger change in frequency is received. Regarding the slope it can be assumed that the more D_2O the faster it goes for the heavier D_2O molecules to exchange the lighter water molecules. When looking at the unexpected behaviour of the b-values it seems to be a peak value in the regions where the D_2O solution is about 50 wt-%, which is a behaviour that is not really explainable at this time. It is also interesting to see that there were differences regarding the fit of the exponential model to the D_2O to H_2O curve. This suggests that the behaviour at that part of the curve is different than going from H_2O to D_2O. These behaviours might have to do

something with how the D_2O molecules bind to the surface. Perhaps that the more D_2O there is the more they associate with the surface and lipid bilayer and consequently make it harder to exchange them. Therefore the model used for fitting the curve does not work for these regions.

During the experiments differences when sonication half of the D_2O solutions before starting the water exchange was investigated, but no differences were observed in the results. This suggests that the D_2O and H_2O in solution mix well even without further stirring.

When observing the bilayers formed with proteoliposomes it did not show the same formation behaviour as for the pure liposome ones. As was seen in Figure 17 it is believed that lipid bilayers are formed also when using proteoliposomes, but that the proteoliposomes that are on the surface collapse only when the fluid was changed to milli-Q water. This is an indication that it is harder for the vesicles to rupture when aquaporins are incorporated in them and that they need some extra force to collapse. When milli-Q water is added it is believed that it increases the osmotic pressure inside the vesicles and causes them to rupture.

A factor that must be taken into consideration regarding the QCM-D results is that lipid bilayers were only formed on one crystal of each mesoporous surfaces at one time, which means that the results are not statistically comparable. Differences in the experimental setup that might give differences in results must also be considered. An example of such a difference is that changing the QCM-D chamber used might give different results since the flow in one chamber might be slightly different from another.

5.3 DLS measurements

The results from the DLS show that the proteoliposomes are bigger than the liposomes. This is an expected result as the lipids are smaller than the aquaporins and therefore can create smaller vesicles. When aquaporins are incorporated they therefore seem to decrease the curvature of the vesicles.

6 Conclusion

From the results obtained in this study it can be concluded that cubic mesoporous silica with ordered regions were successfully made using the three templating molecules P123, BrijS10 and CTAB. The pore sizes fit according to previous studies and the thickness of the films are as expected in the nanometre range.

It can also be concluded that having a mesoporous surface on a QCM-D crystal definitely changes the results obtained from analysis. From the results the kinetics and change in frequency while performing water exchange was seen to change drastically and show different behaviours in respect to D_2O concentration. It was also noticed that the ordering and the accessibility of pores also have a major impact on the out coming results.

Lipid bilayers were formed on all surfaces, however not all of the bilayers were continuous. Lipid bilayers with incorporated aquaporins were also able to form on the mesoporous and non-porous surfaces. From DLS it was determined that the proteoliposomes were bigger than the liposomes.

The results also showed that it is hard to reproduce surfaces with the same mesoporous structure and furthermore more experiments in general need to be performed to get statistical credibility.

7 Future work

It would be interesting to further investigate the different kinetic behaviours that were observed while analysing the QCM-D data. It would also be good to look at other ways to try to make it easier to create lipid bilayers with aquaporins, perhaps ways to increase the osmotic pressure more during the bilayer formation. Another way to decrease the differences between runs in the QCM-D during water exchange with and without bilayer is to conduct the two experiments during the same run; you perform water exchange, form bilayer on the surface and perform water exchange again.

A way to control the synthesis process for the mesoporous silica more might be good, to get more control of the resulting film thickness and porous structure.

8 Bibliography

1. Q-Sense. The QCM-D principle. 2011; http://www.q-sense.com/support-education/faq-qcm-d/the-qcm-d-principle. Accessed May 20, 2014.

2. Wallin M. *Formation of Mesoporous Materials and their use as Lipid Bilayer Supports*: Department of Chemical and Biological Engineering, Chalmers University of Technology; 2014.

3. Tang CY, Zhao Y, Wang R, Hélix-Nielsen C, Fane AG. Desalination by biomimetic aquaporin membranes: Review of status and prospects. *Desalination.* 2013;308:34-40.

4. Claesson M, Frost R, Svedhem S, Andersson M. Pore Spanning Lipid Bilayers on Mesoporous Silica Having Varying Pore Size. *Langmuir.* 2011;27:8974-8982.

5. UNICEF, Organisation WH. Progress on Drinking Water and Sanitaion: 2012 Update. 2012. http://www.unicef.org/media/files/JMPreport2012.pdf.

6. Pendergast MTM, Hoek EMV. A review of water treatment membrane nanotechnologies. *Energy & Environmental Science.* 2011;4:1946-1971.

7. Kumar M, Grzelakowskl M, Zilles J, Clark M, Meler W. Highly permeable polymeric membranes based on the incorporation of the functional water channel protein Aquaporin Z. *Proceedings in of the National Academy of Sciences.* December 26 2007;104(52):20719-20724.

8. Verkman AS. More than just water channels: unexpected cellular roles of aquaporins. *Journal of Cell Science.* 2005;118:3225-3232.

9. Keizer HM, Dorvel BR, Andersson M, et al. Functional Ion Channels in Tethered Bilayer Membranes- Implications for Biosensors. *ChemBioChem.* 2007;8:1246-1250.

10. Andersson M, Okeyo G, Wilson D, et al. Voltage-induced gating of the mechanosensitive MscL ion channel reconstructed in a tethered lipid bilayer membrane. *Biosensors and Bioelectronics.* 2008;23:919-923.

11. Sackmann E. Supported Membranes: Scientific and Practical Applications. *Sceince.* January 5 1996;271:43-48.

12. Sackmann E, Tanaka M. Supported membranes on soft cushions: fabrication, characterization and applications. *Trends in Biotechnology.* 2000;18:58-64.

13. Kaufman Y, Berman A, Freger V. Supported Lipid Bilayer Membranes for Water Purification by Reverse Osmosis. *Langmuir.* 2010;26(10):7388-7395.

14. Claesson M, Cho N-J, Frank CW, Andersson M. Vesicle Adsorption on Mesoporous Silica and Titania. *Langmuir.* 2010;26(22):16630-16633.

15. Alberius PCA, Frindell KL, Hayward RC, Kramer EJ, Stucky GD, Chmelka BF. General Predictive Syntheses of Cubic, Hexagonal, and Lamellar Silica and Titania Mesostructured Thin Films. *Chemistry of Materials.* 2002;14(8):3284-3294.

16. Besson S, Gacoin T, Ricolleau C, Jacuiod C, Boilot J-P. Phase diagram for mesoporous CTAB-silica films prepared under dynamic conditions. *Journal of Materials Chemistry.* 2003;13:404-409.

17. Coquil T, Richman EK, Hutchinson NJ, Tolbert SH, Pilon L. Thermal conductivity of cubic and hexagonal mesoporous silica thin films. *Journal of Applied Physics.* 2009;106.

18. Cademartiri L, Ozin GA. *Concepts of Nanochemistry*. Weinheim: Wiley-VCH; 2009.

19. Zhao D, Yang P, Melosh N, Feng J, Chmelka BF, Stucky GD. Continous Mesoporous Silica Films with Highly Ordered Large Pore Structures. *Advanced Materials.* 1998;10(16):1380-1385.

20. Brinker CJ, Lu Y, Sellinger A, Fan H. Evaporation-Induced Self-Assembly: Nanostructures Made Easy. *Advanced Materials.* 1999;11(7):579-585.

21. Liu S, Cool P, Collart O, et al. The Influence of Alcohol Concentraion on the Structural Ordering of Mesoporous Silica: Cosurfactant versus Cosolvent. *The Journal of Physical Chemistry B.* 2003;107(38):10405-10411.

22. Brinker CJ. Hydrolysis and Condensation of Silicates: Effects on Structure. *Journal of Non-Crystalline Solids.* 1988;100:31-50.

23. Encyclopedia of Neuroscience. In: Binder MD, Hirokawa N, Windhorst U, eds. Berlin: Springers-Verlag GmbH; 2009.

24. Höök F, Rodahl M, Brzezinski P, Kasemo B. Energy Dissipation Kinetics for Protein and Antibody-Antigen Adsorption under Shear Oscillation on a Quartz Crystal Microbalance. *Langmuir.* 1998;14:729-734.

25. Q-Sense. Quartz Crystal Microbalance with Dissipation (QCM-D). 2011. http://www.q-sense.com/qcm-d-technology. Accessed July 13.

26. Edvardsson M, Rodahl M, Kasemo B, Höök F. A Dual-Frequency QCM-D Setup Operating at Elevated Oscillation Amplitudes. *Analytical Chemistry.* August 1 2005;77(15):4918-4926.

27. Reimer L, Kohl H. *Transmission Electron Microscopy: Physics of Image Formation*. New York: Springer; 2008.

28. Reimer L. *Scanning Electron Microscopy: Physics of Image Formation and Microanalysis*. New York: Springer; 1998.

29. Ltd MI. Dynamic Light Scattering (DLS). 2014; http://www.malvern.com/en/products/technology/dynamic-light-scattering/. Accessed March 17, 2014.

30. Laborador A, Cerenius Y, Svensson C, Theodor K, Plivelic T. The yellow mini-hutch for SAXS experiments at MAX IV Laboratory. *Journal of Physics: Conference Series.* 2013;425.

31. Keller CA, Kasemo B. Surface Specific Kinetics of Lipid Vesicle Adsorption Measured with a Quartz Crystal Microbalance. *Biophysical Journal.* 1998;75:1397-1402.

32. Morell J, Güngerich M, Wolter G, et al. Synthesis and characterization of highly ordered bifunctional aromatic periodic mesoporous organosilicas with different pore sizes. *Journal of Materials Chemistry.* 2006;16:2809-2818.

9 Appendix

The frequency change, the value of the slope, the calculated volume and percentage of D_2O in the mesoporous network and the b-values from the different QCM-D measurements are found in the figures below. The data marked in yellow are for values that were hard to fit to the exponential model or were else hard to compare with other values. The data marked in green were data that were hard to measure due to strange frequency behavior. In Table A1 information can be found about which data in each figure below that belong to which type of experiments.

Table A1 - Table of the different fluids used during QCM-D analysis for the different experiments. H_2O and D_2O exchange were conducted during all experiments.

Figure number	Liposomes	Proteoliposomes
A1	-	-
A2	-	-
A3	-	-
A4	-	-
A5	Yes	-
A6	Yes	-
A7	Yes	-
A8		Yes

Sample	wt-% D2O	Δf H2O-D2O (Hz)	Δf D2O-H2O (Hz)	Slope H2O-D2O	Slope D2O-H2O	VH2O (mL)	VH2O/Vfilm (%)	b-value H2O->D2O	b-value D2O->H2O
Reference 4:1	5%	-7,99	-3,1182	-0,0514	0,0753			0,01255	0,02947
Reference 4:1	5%	-6,09	-3,2416	-0,0641	0,0594			0,02473	0,02452
Reference 4:1	5%	-3,987	-4,0634	-0,0376	0,0786			0,02796	0,02636
Reference 4:1	5%	-3,873	-4,0853	-0,0545	0,0618			0,02079	0,02907
Reference 4:1	40%	-30,556	-30,5937	-0,627	0,547			0,04875	0,05624
Reference 4:1	40%	-30,426	-30,5164	-0,6169	0,5372			0,04913	0,05917
Reference 4:1	40%	-30,722	-30,6835	-0,6329	0,5512			0,05173	0,0555
Reference 4:1	40%	-30,512	-30,5909	-0,6107	0,6259			0,04993	0,05621
Reference 4:1	60%	-45,423	-45,5481	-0,8788	0,7946			0,05343	0,05543
Reference 4:1	60%	-45,478	-45,4127	-0,8913	0,7376			0,05209	0,05995
Reference 4:1	60%	-45,583	-45,609	-0,8425	0,7288			0,05159	0,05704
Reference 4:1	60%	-45,534	-45,6026	-0,9006	0,7803			0,05199	0,05812
Reference 4:1	99,90%	-76,884	-76,9074	-1,3634	0,9825			0,0469	0,0475
Reference 4:1	99,90%	-76,723	-76,6046	-1,3062	1,195			0,04368	0,05635
Reference 4:1	99,90%	-76,888	-77,0463	-1,3863	1,0733			0,04924	0,05905
Reference 4:1	99,90%	-76,363	-76,1656	-1,2698	1,036			0,04864	0,06029
P123 6:2	5%	-9,064	-9,2149	-0,1217	0,1411			0,04739	0,04353
P123 6:2	5%	-9,231	-9,1922	-0,1457	0,1227			0,04187	0,04118
P123 6:2	5%	-9,275	-9,1085	-0,1702	0,1757			0,05024	0,04374
P123 6:2	5%	-9,198	-9,182	-0,1291	0,1592			0,04496	0,04015
P123 6:2	40%	-70,354	-69,6475	-1,6289	1,3756			0,06342	0,0664
P123 6:2	40%	-69,517	-69,7766	-1,6497	1,3318			0,06443	0,06206
P123 6:2	40%	-70,929	-70,1981	-1,4504	1,4208			0,06171	0,06293
P123 6:2	40%	-69,801	-70,0338	-1,5962	1,4867			0,06198	0,06579
P123 6:2	60%	-104,668	-104,4852	-2,1278	1,8967			0,05593	0,06602
P123 6:2	60%	-104,324	-104,648	-2,431	1,9254			0,05712	0,0669
P123 6:2	60%	-104,7	-104,8149	-1,9727	1,9376			0,05566	0,06626
P123 6:2	60%	-104,436	-104,9826	-1,967	2,0093			0,0536	0,06626
P123 6:2	99,90%	-177,37	-177,349	-3,5761	2,9439	2,78512E-06	19,1062649	0,05003	0,06182
P123 6:2	99,90%	-176,52	-176,6385	-3,3924	3,0029	2,76602E-06	18,97525943	0,05098	0,06082
P123 6:2	99,90%	-176,838	-178,1639	-3,6072	2,9211	2,77026E-06	19,00435063	0,04508	0,06117
P123 6:2	99,90%	-176,292	-176,4235	-3,5937	3,0211	2,76968E-06	19,00035772	0,05071	0,06186

Figure A1 – Data from the QCM-D analysis where H_2O and D_2O exchange where performed. Yellow data were hard to fit to exponential model and green data was hard to measure. Data from the P123 crystal 6:2 and reference crystal 4:1 are found here.

Sample	wt-% D2O	Δ_f H2O-D2O (Hz)	Δ_f D2O-H2O (Hz)	Slope H2O-D2O	Slope D2O-H2O	VH2O (mL)	VH2O/Vfilm (%)	b-value H2O->D2O	b-value D2O->H2O
BrijS10 6:3	5%	-4,358	-4,4177	-0,0637	0,0609			0,02185	0,0224
BrijS10 6:3	5%	-4,2206	-4,2183	-0,0656	0,0692			0,02452	0,0271
BrijS10 6:3	5%	-4,328	-4,1424	-0,0486	0,0349			0,02358	0,01981
BrijS10 6:3	5%	-4,34	-4,2322	-0,0386	0,0474			0,02415	0,02206
BrijS10 6:3	40%	-33,642	-33,5932	-0,5555	0,6352			0,04583	0,04695
BrijS10 6:3	40%	-33,278	-33,3851	-0,5424	0,5672			0,04804	0,04809
BrijS10 6:3	40%	-33,693	-33,4708	-0,5596	0,5799			0,04665	0,04801
BrijS10 6:3	40%	-33,236	-33,5093	-0,6829	0,5741			0,04774	0,04844
BrijS10 6:3	60%	-51,81	-51,907	-1,0118	0,8371			0,04854	0,05236
BrijS10 6:3	60%	-51,829	-52,0231	-0,9115	0,9492			0,04608	0,04944
BrijS10 6:3	60%	-52,121	-52,1077	-0,9117	0,8788			0,04803	0,05193
BrijS10 6:3	60%	-51,916	-52,1009	-0,9129	0,9026			0,04654	0,05001
BrijS10 6:3	99,90%	-87,998	-87,7452	-1,4154	1,2378	3,08041E-07		0,04834	0,04505
BrijS10 6:3	99,90%	-87,411	-87,437	-1,2313	1,2261	2,96234E-07		0,04444	0,04469
BrijS10 6:3	99,90%	-87,671	-87,5431	-1,4404	1,2528	2,98867E-07		0,04569	0,0444
BrijS10 6:3	99,90%	-87,072	-86,9987	-1,3605	1,1953	2,96816E-07		0,04857	0,04166
CTAB 6:4	5%	-5,426	-5,5542	-0,0572	0,0738			0,03421	0,03814
CTAB 6:4	5%	-5,327	-5,5288	-0,0752	0,0629			0,04168	0,03596
CTAB 6:4	5%	-5,328	-5,3521	-0,0558	0,0258			0,03303	0,03447
CTAB 6:4	5%	-5,354	-5,4039	-0,1166	0,0896			0,03412	0,0343
CTAB 6:4	40%	-45,057	-44,8135	-0,9795	0,9028			0,05791	0,05623
CTAB 6:4	40%	-44,287	-44,7829	-0,9036	0,9342			0,05839	0,0591
CTAB 6:4	40%	-45,416	-45,1278	-0,833	0,9371			0,05796	0,05944
CTAB 6:4	40%	-44,598	-44,9995	-0,8377	0,8294			0,06086	0,05999
CTAB 6:4	60%	-68,757	-68,8614	-1,2429	1,4722			0,05908	0,06201
CTAB 6:4	60%	-68,394	-68,9326	-1,4476	1,3427			0,05885	0,06246
CTAB 6:4	60%	-68,868	-69,1314	-1,4139	1,4507			0,05737	0,06182
CTAB 6:4	60%	-68,424	-69,3183	-1,4843	1,3935			0,05985	0,06293
CTAB 6:4	99,90%	-117,634	-117,3201	-2,0623	2,0961	1,12945E-06	7,748146955	0,05593	0,05634
CTAB 6:4	99,90%	-116,622	-117,7167	-2,2577	2,1912	1,10586E-06	7,586339027	0,05825	0,06098
CTAB 6:4	99,90%	-117,214	-117,9612	-2,4224	1,9526	1,11769E-06	7,667528199	0,05519	0,05913
CTAB 6:4	99,90%	-116,65	-117,2292	-2,0676	2,1479	1,11661E-06	7,660112794	0,05754	0,05935

Figure A2 – Data from the QCM-D analysis where H_2O and D_2O exchange were performed. Data from the BrijS10 crystal 6:3 and CTAB crystal 6:4 are found here.

Sample	wt-% D2O	Δ_f H2O-D2O (Hz)	Δ_f D2O-H2O (Hz)	Slope H2O-D2O	Slope D2O-H2O	VH_2O (mL)	VH_2O/V_{film} (%)	b-value H2O->D2O	b-value D2O->H2O
Reference 4:1	5%	-3,702	-4,1928	-0,0331	0,0475			0,02386	0,02893
Reference 4:1	5%	-3,807	-4,0871	-0,0357	0,0822			0,01888	0,03035
Reference 4:1	5%	-3,723	-3,9506	-0,1172	0,0525			0,02619	0,02582
Reference 4:1	5%	-3,832	-3,9793	-0,0442	0,0918			0,02731	0,02946
Reference 4:1	40%	-30,929	-30,8075	-0,6345	0,6193			0,05057	0,0494
Reference 4:1	40%	-30,91	-30,9363	-0,6792	0,5973			0,05114	0,0473
Reference 4:1	40%	-30,783	-30,8991	-0,6687	0,5811			0,05301	0,04846
Reference 4:1	40%	-29,845	-29,8402	-0,6018	0,478			0,05489	0,04602
Reference 4:1	60%	-46,31	-46,4952	-0,7861	0,7869			0,05484	0,04816
Reference 4:1	60%	-46,396	-46,2473	-0,9417	0,7897			0,05189	0,04872
Reference 4:1	60%	-46,26	-46,3769	-0,9625	0,774			0,05291	0,04928
Reference 4:1	60%	-46,299	-46,4346	-0,9989	0,7974			0,05365	0,0506
Reference 4:1	99,90%	-77,171	-77,1872	-1,5211	1,2957			0,04978	0,04353
Reference 4:1	99,90%	-77,067	-77,0234	-1,3568	1,2192			0,0483	0,04554
Reference 4:1	99,90%	-77,137	-77,1351	-1,4315	1,147			0,0458	0,04534
Reference 4:1	99,90%	-77,004	-77,0596	-1,5014	1,1604			0,04648	0,04512
P123 5:4	5%	-10,031	-9,8269	-0,1339	0,1408			0,04612	0,04285
P123 5:4	5%	-9,843	-10,1254	-0,1249	0,1255			0,04567	0,05512
P123 5:4	5%	-9,618	-9,8594	-0,2341	0,1443			0,04451	0,04697
P123 5:4	5%	-9,531	-9,7904	-0,1668	0,0946			0,0535	0,03233
P123 5:4	40%	-74,286	-73,9094	-1,5695	1,3948			0,06372	0,06028
P123 5:4	40%	-73,475	-73,9582	-1,5469	1,4651			0,05877	0,0638
P123 5:4	40%	-73,695	-73,9356	-1,6254	1,361			0,05942	0,06414
P123 5:4	40%	-71,143	-71,5045	-1,4891	1,2588			0,06165	0,0616
P123 5:4	60%	-112,95	-112,3723	-2,6048	1,9227			0,05378	0,06261
P123 5:4	60%	-111,07	-112,632	-2,2489	1,9491			0,05694	0,06328
P123 5:4	60%	-113,037	-113,6819	-2,245	2,1395			0,05821	0,06194
P123 5:4	60%	-112,517	-113,3235	-2,048	2,0991			0,05116	0,06196
P123 5:4	99,90%	-186,915	-190,1049	-4,1722	3,354	3,04172E-06	20,86656784	0,05196	0,06274
P123 5:4	99,90%	-187,745	-189,5303	-3,5053	3,1817	3,0676E-06	21,04415727	0,04921	0,05811
P123 5:4	99,90%	-189,388	-189,4456	-3,8873	2,964	3,1112E-06	21,34324525	0,04598	0,06032
P123 5:4	99,90%	-188,621	-190,0762	-4,4631	3,2801	3,09363E-06	21,22269739	0,04579	0,05783

Figure A3 – Data from the QCM-D analysis where H_2O and D_2O exchange were performed. Data from the P123 crystal 5:4 and reference crystal 4:1 are found here.

Sample	wt-% D2O	Δ_f H2O-D2O (Hz)	Δ_f D2O-H2O (Hz)	Slope H2O-D2O	Slope D2O-H2O	V_{H2O} (mL)	V_{H2O}/V_{film} (%)	b-value H2O->D2O	b-value D2O->H2O
BrijS10 5:5	5%	-6,349	-6,6922	-0,0943	0,0678			0,03527	0,03137
BrijS10 5:5	5%	-6,177	-6,7212	-0,0954	0,1052			0,02975	0,03505
BrijS10 5:5	5%	-6,112	-6,4337	-0,0624	0,0891			0,03068	0,02907
BrijS10 5:5	5%	-6,202	-6,4346	-0,071	0,065			0,03417	0,03366
BrijS10 5:5	40%	-50,942	-50,8831	-0,8933	0,9341			0,04985	0,05441
BrijS10 5:5	40%	-50,616	-50,8504	-1,0316	0,8758			0,04836	0,05322
BrijS10 5:5	40%	-50,557	-50,6617	-0,9964	0,9298			0,04993	0,04812
BrijS10 5:5	40%	-49,139	-49,2139	-0,7687	0,9382			0,04905	0,04923
BrijS10 5:5	60%	-76,992	-76,588	-1,3873	1,2916			0,04438	0,05161
BrijS10 5:5	60%	-75,837	-76,5112	-1,2865	1,3051			0,05154	0,05058
BrijS10 5:5	60%	-77,179	-76,9816	-1,095	1,1959			0,04055	0,0498
BrijS10 5:5	60%	-75,788	-77,0531	-1,3226	1,2877			0,04284	0,05045
BrijS10 5:5	99,90%	-128,598	-129,662	-2,0592	1,788	1,42538E-06		0,04121	0,04441
BrijS10 5:5	99,90%	-129,477	-129,5179	-2,3376	1,8272	1,45262E-06		0,03904	0,04363
BrijS10 5:5	99,90%	-130,04	-129,6182	-2,5391	1,9578	1,46628E-06		0,04041	0,04364
BrijS10 5:5	99,90%	-129,24	-129,5859	-2,1657	1,786	1,4478E-06		0,04022	0,04314
CTAB 6:1	5%	-8,596	-8,7204	-0,1074	0,1282			0,04749	0,04103
CTAB 6:1	5%	-8,051	-8,4758	-0,1203	0,1614			0,04277	0,0351
CTAB 6:1	5%	-8,169	-8,3014	-0,1178	0,107			0,04251	0,0407
CTAB 6:1	5%	-8,067	-8,0859	-0,1381	0,1115			0,03931	0,04422
CTAB 6:1	40%	-61,282	-60,709	-1,2189	1,0011			0,05734	0,05882
CTAB 6:1	40%	-60,633	-60,8988	-1,2602	1,0977			0,05669	0,05949
CTAB 6:1	40%	-60,723	-60,6149	-1,2346	1,2093			0,05584	0,05679
CTAB 6:1	40%	-58,821	-58,6657	-1,1638	1,0784			0,05569	0,05633
CTAB 6:1	60%	-92,799	-92,2748	-1,7349	1,5449			0,0568	0,05764
CTAB 6:1	60%	-91,752	-92,4074	-1,91	1,5788			0,06681	0,05656
CTAB 6:1	60%	-94,191	-93,2586	-1,948	1,637			0,05426	0,05546
CTAB 6:1	60%	-92,573	-93,0677	-2,0183	1,6155			0,05664	0,05706
CTAB 6:1	99,90%	-154,546	-157,3596	-3,4004	2,3603	2,14456E-06	14,71197228	0,05133	0,04905
CTAB 6:1	99,90%	-156,569	-156,9042	-2,9741	2,4709	2,20352E-06	15,11639704	0,05003	0,04967
CTAB 6:1	99,90%	-157,608	-156,8	-2,9907	2,6559	2,23037E-06	15,30064131	0,05161	0,03971
CTAB 6:1	99,90%	-156,536	-156,6468	-2,9729	2,4269	2,20435E-06	15,12210119	0,05424	0,05319

Figure A4 – Data from the QCM-D analysis where H_2O and D_2O exchange were performed. Yellow data were hard to fit to exponential model. Data from the BrijS10 crystal 5:5 and CTAB crystal 6:1 are found here.

Sample	wt-% D2O	Δ_f H2O-D2O (Hz)	Δ_f D2O-H2O (Hz)	Slope H2O-D2O	Slope D2O-H2O	VH2O (mL)	VH2O/Vfilm (%)	b-value H2O->D2O	b-value D2O->H2O
Reference 4:1	5%	-1,979	-4,5608	-0,0655	0,0612			0,02579	0,02864
Reference 4:1	5%	-3,072	-4,1233	-0,0543	0,0771			0,0234	0,02612
Reference 4:1	40%	-28,493	-29,2513	0,6041	0,6255			0,05112	0,06531
Reference 4:1	40%	-27,77	-28,9318	-0,6451	0,6459			0,05197	0,06029
Reference 4:1	60%	-42,361	-43,1657	-0,8759	0,7877			0,05481	0,06435
Reference 4:1	60%	-42,189	-43,004	-0,9345	0,9057			0,05747	0,06334
Reference 4:1	99,90%	-67,718	-68,7475	-1,6499	1,2467			0,05652	0,05996
Reference 4:1	99,90%	-67,574	-68,7221	-1,7106	1,2831			0,05584	0,05868
P123 5:4	5%	-8,794	-10,8309	-0,2251	0,1783			0,04796	
P123 5:4	5%	-10,101	-10,8925	-0,2015	0,1813			0,04851	
P123 5:4	40%	-79,459	-80,1231	-1,7702	1,4748			0,06894	0,06886
P123 5:4	40%	-78,535	-80,2184	-1,8448	1,5638			0,07082	0,06986
P123 5:4	60%	-120,218	-121,7975	-2,6326	2,2204			0,06381	0,06657
P123 5:4	60%	-119,607	-122,227	-2,9086	2,2635			0,06663	0,06342
P123 5:4	99,90%	-198,795	-203,111	-4,4873	3,5171	3,63299E-06	24,92279407	0,05258	0,0663
P123 5:4	99,90%	-198,727	-202,6474	-4,5691	3,3094	3,6351E-06	24,9372446	0,04494	0,06443
BrijS10 5:5	5%	-6,093	-6,9507	-0,1128	0,1159			0,0426	
BrijS10 5:5	5%	-6,153	-6,9255	-0,1044	0,1146			0,0403	
BrijS10 5:5	40%	-49,979	-50,7901	-1,0586	1,0248			0,06314	0,0671
BrijS10 5:5	40%	-49,227	-50,6822	-1,1008	1,0465			0,06402	0,06641
BrijS10 5:5	60%	-74,003	-75,2415	-1,6922	1,5304			0,05743	0,06383
BrijS10 5:5	60%	-73,041	-75,8155	-1,778	1,4217			0,06077	
BrijS10 5:5	99,90%	-127,324	-130,2677	-2,6447	2,1212	1,65207E-06		0,05462	
BrijS10 5:5	99,90%	-127,174	-129,7092	-2,8022	2,1686	1,6519E-06		0,0534	
CTAB 6:1	5%	-6,239	-8,9649	-0,1006	0,129			0,042	
CTAB 6:1	5%	-8,07	-8,7609	-0,1234	0,1077			0,03352	
CTAB 6:1	40%	-67,373	-68,1859	-1,3506	1,1873			0,05576	
CTAB 6:1	40%	-66,895	-68,1501	-1,2498	1,218			0,05493	
CTAB 6:1	60%	-101,321	-102,9042	-1,9493	1,7497			0,08724	0,04709
CTAB 6:1	60%	-100,383	-103,1411	-1,9964	1,769			0,05015	0,05953
CTAB 6:1	99,90%	-168,342	-173,025	-3,1693	2,6486	2,78894E-06	19,13250403	0,04108	0,0245
CTAB 6:1	99,90%	-168,029	-172,2038	-2,8749	2,6846	2,78426E-06	19,10037061	0,04315	0,05244

Figure A5 – Data from the QCM-D analysis where H_2O and D_2O exchange were performed with crystals covered with liposomes. Yellow data were hard to fit to exponential model. Bilayers from this analysis were formed on the BrijS10 and CTAB samples. Data from the Reference crystal 4:1, P123 crystal 5:4, BrijS10 crystal 5:5 and CTAB crystal 6:1 are found here.

Sample	wt-% D2O	Δ_f H2O-D2O (Hz)	Δ_f D2O-H2O (Hz)	Slope H2O-D2O	Slope D2O-H2O	VH_2O (mL)	VH_2O/V_{film} (%)	b-value H2O->D2O	b-value D2O->H2O
Reference 4:1	5%	-3,144	-4,1332	-0,0724	0,0867			0,02433	0,03047
Reference 4:1	5%	-2,72	-4,6073	-0,0498	0,0567			0,02406	0,02366
Reference 4:1	40%	-26,812	-28,6422	-0,5	0,5132			0,03814	0,04792
Reference 4:1	40%	-27,177	-27,9378	-0,7277	0,4973			0,05046	0,04661
Reference 4:1	60%	-40,28	-40,806	-0,8665	0,7022			0,0566	0,05306
Reference 4:1	60%	-40,193	-40,9008	-0,873	0,6923			0,05721	0,05376
Reference 4:1	99,90%	-65,717	-66,0853	-1,5039	0,9038			0,04835	0,04862
Reference 4:1	99,90%	-65,674	-64,5763	-1,4054	0,8646			0,04845	0,05007
P123 6:2	5%	-9,127	-10,0072	-0,17	0,1428			0,04326	0,04768
P123 6:2	5%	-8,967	-9,8417	-0,1656	0,149			0,03879	0,04892
P123 6:2	40%	-69,493	-69,5851	-1,6373	1,423			0,06509	0,07125
P123 6:2	40%	-69,058	-69,8735	-1,6088	1,5063			0,06809	0,07161
P123 6:2	60%	-103,309	-104,2272	-2,4893	2,0131			0,06486	0,07019
P123 6:2	60%	-103,206	-104,3601	-2,4968	2,052			0,06502	0,06436
P123 6:2	99,90%	-174,2	-175,3386	-3,7051	2,9948	3,00677E-06	20,62680309	0,06498	0,06143
P123 6:2	99,90%	-173,958	-175,3993	-3,8317	2,5833	3,00125E-06	20,58896552	0,05372	0,06022
CTAB 6:4	5%	-5,107	-5,7978	-0,0891	0,0799			0,03633	0,04431
CTAB 6:4	5%	-5,159	-5,7858	-0,1011	0,0748			0,3388	0,03622
CTAB 6:4	40%	-44,197	-44,7753	-0,9014	0,8404			0,05308	0,05733
CTAB 6:4	40%	-43,964	-44,9351	-0,8656	0,8341			0,05385	
CTAB 6:4	60%	-66,069	-67,025	-1,3976	1,1988			0,05455	0,0632
CTAB 6:4	60%	-65,967	-67,1328	-1,3613	0,1903			0,05713	0,05794
CTAB 6:4	99,90%	-110,702	-111,8872	-2,2936	1,7699	1,24683E-06	11,27491504	0,05282	0,05503
CTAB 6:4	99,90%	-110,617	-112,1082	-2,3333	1,7577	1,24566E-06	11,26438828	0,05906	0,0522
P123 5:3	5%	-10,323	-10,7614	-0,2106	0,1625			0,04884	
P123 5:3	5%	-10,074	-10,7874	-0,1825	0,1868			0,04692	
P123 5:3	40%	-81,296	-81,6545	-1,7703	1,679			0,06905	0,07024
P123 5:3	40%	-81,006	-81,8138	-1,8145	1,626			0,07091	0,06715
P123 5:3	60%	-121,834	-122,8304	-2,952	2,5129			0,06423	0,07011
P123 5:3	60%	-121,758	-123,0506	-2,9706	2,5209			0,06296	0,07406
P123 5:3	99,90%	-202,942	-204,4602	-4,4491	3,7766	3,80339E-06	26,09176603	0,05777	0,07208
P123 5:3	99,90%	-202,744	-204,4677	-4,4633	3,7065	3,7991E-06	26,06229455	0,06008	0,06438

Figure A6 – Data from the QCM-D analysis where H_2O and D_2O exchange with crystals covered with liposomes. Yellow data were hard to fit to exponential model and green data were hard to measure. Lipid bilayer was formed on P123 crystal 6:2 during this analysis. Data from the P123 crystals 5:3 and 6:2, reference crystal 4:1 and CTAB 6:4 are found here.

Sample	wt-% D2O	Δ_f H2O-D2O (Hz)	Δ_f D2O-H2O (Hz)	Slope H2O-D2O	Slope D2O-H2O	V_{H2O} (mL)	V_{H2O}/V_{film} (%)	b-value H2O->D2O	b-value D2O->H2O
Reference 4:1	5%	-3,2589	-3,4726	-0,0457	0,0716			0,02074	0,02056
Reference 4:1	5%	-3,2628	-3,4244	-0,0667	0,0393			0,02268	0,02178
Reference 4:1	40%	-28,692	-28,8216	-0,5695	0,5761			0,05183	0,06783
Reference 4:1	40%	-28,6672	-28,8122	-0,5522	0,611			0,05249	0,067
Reference 4:1	60%	-42,523	-42,5731	-0,9586	0,8794			0,05395	0,06237
Reference 4:1	60%	-42,494	-42,5891	-0,8912	0,8503			0,05688	0,0615
Reference 4:1	99,90%	-70,734	-70,844	-1,1501	1,1282			0,0534	0,06144
Reference 4:1	99,90%	-70,587	-70,745	-1,2097	1,1143			0,05354	0,06098
P123 6:2	5%	-11,321	-11,5299	-0,1672	0,184			0,05359	
P123 6:2	5%	-11,184	-11,5511	-0,144	0,1793			0,06044	
P123 6:2	40%	-89,1917	-89,5137	-1,5803	1,4317			0,06944	0,07011
P123 6:2	40%	-88,772	-89,6605	-1,6807	1,5688			0,06865	0,06792
P123 6:2	60%	-131,972	-133,1246	-2,5593	2,1849			0,06479	0,07173
P123 6:2	60%	-132,069	-133,0419	-2,4206	2,2012			0,0623	0,07205
P123 6:2	99,90%	-219,959	-221,0486	-3,6278	3,3763	4,13599E-06	28,37342894	0,0513	
P123 6:2	99,90%	-219,726	-220,7101	-3,6636	3,4666	4,13361E-06	28,35707702	0,05485	
BrijS10 5:5	5%	-5,492	-5,4827	-0,0832	0,0643			0,03051	
BrijS10 5:5	5%	-5,296	-5,52	-0,0728	0,0645			0,03362	
BrijS10 5:5	40%	-34,14	-34,0785	-0,7321	0,78			0,06202	0,05476
BrijS10 5:5	40%	-34,069	-34,1857	-0,7193	0,6254			0,05965	0,08391
BrijS10 5:5	60%	-49,412	-49,8553	-1,0793	0,9884			0,06379	0,07349
BrijS10 5:5	60%	-49,549	-49,7114	-1,015	1,0198			0,06259	0,07501
BrijS10 5:5	99,90%	-81,543	-81,4991	-1,6481	1,3099	2,99587E-07		0,05973	0,05854
BrijS10 5:5	99,90%	-81,255	-81,3284	-1,6264	1,4302	2,95679E-07		0,06058	0,07482
CTAB 6:1	5%	-5,3136	-5,5931	-0,0881	0,0719			0,02894	0,05108
CTAB 6:1	5%	-5,298	-5,6778	-0,0652	0,0703			0,02587	0,02911
CTAB 6:1	40%	-37,9158	-38,0106	-0,5716	0,635			0,04515	
CTAB 6:1	40%	-37,8719	-38,1971	-0,5945	0,608			0,04566	
CTAB 6:1	60%	-56,76	-57,0627	-0,9712	1,0561			0,04347	
CTAB 6:1	60%	-56,753	-57,0479	-0,8794	0,9738			0,04288	
CTAB 6:1	99,90%	-95,545	-96,0391	-1,6605	1,2923	6,87674E-07	4,717528199	0,04331	
CTAB 6:1	99,90%	-95,653	-95,9278	-1,519	1,4616	6,94741E-07	4,766013535	0,04164	

Figure A7 – Data from the QCM-D analysis where H_2O and D_2O exchange were performed with crystals covered with liposomes. Yellow data were hard to fit to exponential model. Bilayer from this analysis was formed on the non-porous reference. Data from the Reference crystal 4:1, P123 crystal 6:2, BrijS10 crystal 5:5 and CTAB crystal 6:1 are found here.

Sample	wt-% D2O	Δf H2O-D2O (Hz)	Δf D2O-H2O (Hz)	Slope H2O-D2O	Slope D2O-H2O	VH2O (mL)	VH2O/Vfilm (%)	b-value H2O->D2O	b-value D2O->H2O
Reference 4:1	5%	-3,583	-3,6861	-0,0592	0,0564			0,02445	0,02335
Reference 4:1	5%	-3,475	-3,6294	-0,0559	0,0421			0,02437	0,02301
Reference 4:1	40%	-29,731	-29,5986	-0,5445	0,4684			0,04715	0,05066
Reference 4:1	40%	-29,642	-29,6426	-0,5789	0,4527			0,04997	0,05002
Reference 4:1	60%	-43,872	-43,8996	-0,8049	0,7455			0,04705	0,05699
Reference 4:1	60%	-43,89	-43,9483	-0,835	0,7374			0,04374	0,0565
Reference 4:1	99,90%	-71,388	-71,3658	-1,3136	1,0198			0,03911	0,05481
Reference 4:1	99,90%	-71,228	-71,4257	-1,3794	0,9342			0,04037	0,05609
P123 6:2	5%	-10,169	-10,5614	-0,1875	0,1786			0,05136	
P123 6:2	5%	-10,206	-10,4781	-0,1893	0,1652			0,0485	
P123 6:2	40%	-80,45	-80,0183	-1,9076	1,5914			0,06962	0,06793
P123 6:2	40%	-79,923	-80,2265	-1,8439	1,7003			0,06983	0,07166
P123 6:2	60%	-119,949	-120,4716	-2,8447	2,1177			0,07148	0,06764
P123 6:2	60%	-119,801	-120,7001	-2,8002	2,2689			0,07438	0,0669
P123 6:2	99,90%	-199,512	-200,6785	-5,0297	3,4446	3,55115E-06	24,36131486	0,06895	0,06746
P123 6:2	99,90%	-199,342	-200,6386	-4,6863	3,4552	3,55087E-06	24,35941347	0,06853	0,06852
BrijS10 5:5	5%	-4,535	-6,0305	-0,0626	0,0787			0,03108	0,03526
BrijS10 5:5	5%	-5,405	-5,8632	-0,1181	0,1019			0,04019	0,0315
BrijS10 5:5	40%	-46,878	-46,8144	-0,9003	0,8259			0,05502	0,06037
BrijS10 5:5	40%	-46,094	-46,881	-0,8618	0,8188			0,05473	0,05603
BrijS10 5:5	60%	-68,829	-69,7459	-1,3105	1,1976			0,05882	0,05464
BrijS10 5:5	60%	-68,8	-69,7253	-1,3331	1,2187			0,05264	0,05306
BrijS10 5:5	99,90%	-116,171	-117,2434	-2,4105	1,7583	1,24123E-06		0,05313	0,04999
BrijS10 5:5	99,90%	-115,942	-117,1477	-2,2629	1,785	1,23931E-06		0,0596	0,04996
CTAB 6:1	5%	-3,232	-6,9698	-0,06	0,1497			0,03689	0,05155
CTAB 6:1	5%	-5,164	-7,028	-0,0127	0,146			0,03826	0,04494
CTAB 6:1	40%	-40,357	-38,841	-0,8139	0,8852			0,06098	0,05921
CTAB 6:1	40%	-38,743	-38,8217	-0,8817	0,811			0,06085	0,05841
CTAB 6:1	60%	-58,537	-58,7374	-1,228	1,1382			0,05511	0,06164
CTAB 6:1	60%	-59,154	-58,8225	-1,2982	1,1048			0,05489	0,06108
CTAB 6:1	99,90%	-101,359	-101,2718	-2,1244	1,6763	8,30691E-07	5,698643248	0,05746	0,05526
CTAB 6:1	99,90%	-101,35	-101,4084	-2,0427	1,6818	8,34876E-07	5,727354173	0,05779	0,05642

Figure A8 - Data from the QCM-D analysis where H_2O and D_2O exchange were performed with crystals covered with proteoliposomes. Yellow data were hard to fit to exponential model and green data was hard to measure. Data from the Reference crystal 4:1, P123 crystal 6:2, BrijS10 crystal 5:5 and CTAB crystal 6:1 are found here.